Toxicology 483 (2023) 153371

Contents lists available at ScienceDirect

Toxicology

journal homepage: www.elsevier.com/locate/toxicol

Sexually concordant and dimorphic transcriptional responses to maternal trichloroethylene and/or N-acetyl cysteine exposure in Wistar rat placental tissue

Elana R. Elkin [a,1,*], Anthony L. Su [a,2], John F. Dou [b,3], Justin A. Colacino [a,c,4], Dave Bridges [c,5], Vasantha Padmanabhan [a,c,d,e,6], Sean M. Harris [a,7], Erica Boldenow [f,8], Rita Loch-Caruso [a,9], Kelly M. Bakulski [b,10]

[a] Department of Environmental Health Sciences, University of Michigan, Ann Arbor, MI, USA
[b] Department of Epidemiology, University of Michigan, Ann Arbor, MI, USA
[c] Department of Nutritional Sciences, University of Michigan, Ann Arbor, MI, USA
[d] Department of Pediatrics, Michigan Medicine, Ann Arbor, MI, USA
[e] Department of Obstetrics and Gynecology, Michigan Medicine, Ann Arbor, MI, USA
[f] Department of Biology, Calvin University, Grand Rapids, MI, USA

ARTICLE INFO

Keywords:
Trichloroethylene
Reproductive toxicology
Placenta
Transcriptomics

ABSTRACT

Numerous Superfund sites are contaminated with the volatile organic chemical trichloroethylene (TCE). In women, exposure to TCE in pregnancy is associated with reduced birth weight. Our previous study reported that TCE exposure in pregnant rats decreased fetal weight and elevated oxidative stress biomarkers in placentae, suggesting placental injury as a potential mechanism of TCE-induced adverse birth outcomes. In this study, we investigated if co-exposure with the antioxidant N-acetylcysteine (NAC) attenuates TCE exposure effects on RNA expression. Timed-pregnant Wistar rats were exposed orally to 480 mg TCE/kg/day on gestation days 6–16. Exposure of 200 mg NAC/kg/day alone or as a pre/co-exposure with TCE occurred on gestation days 5–16 to stimulate antioxidant genes prior to TCE exposure. Tissue was collected on gestation day 16. In male and female placentae, we evaluated TCE- and/or NAC-induced changes to gene expression and pathway enrichment analyses using false discovery rate (FDR) and fold-change criteria. In female placentae, exposure to TCE caused significant differential expression 129 genes while the TCE+NAC altered 125 genes, compared with controls (FDR$<$ 0.05 + fold-change $>$1). In contrast, in male placentae TCE exposure differentially expressed 9 genes and TCE+NAC differentially expressed 35 genes, compared with controls (FDR$<$ 0.05 + fold-change $>$1). NAC alone did not significantly alter gene expression in either sex. Differentially expressed genes observed with TCE exposure were enriched in mitochondrial biogenesis and oxidative phosphorylation pathways in females whereas immune system pathways and endoplasmic reticulum stress pathways were differentially expressed in both sexes (FDR$<$0.05). TCE treatment was differentially enriched for genes regulated by the transcription factors ATF6 (both sexes) and ATF4 (males only), indicating a cellular condition triggered by misfolded proteins during

* Correspondence to: Department of Environmental Health Sciences, University of Michigan, 1415 Washington Heights, Ann Arbor, MI, USA.
E-mail address: elkinela@umich.edu (E.R. Elkin).
[1] ORCID: 0000-0001-8637-1731
[2] ORCID: 0000-0002-5280-6423
[3] ORCID: 0000-0003-4577-8660
[4] ORCID: 0000-0002-5882-4569
[5] ORCID: 0000-0002-5334-972X
[6] ORCID: 0000-0002-8443-7212
[7] ORCID: 0000-0001-9852-7270
[8] ORCID: 0000-0002-3160-5454
[9] ORCID: 0000-0002-5993-2799
[10] ORCID: 0000-0002-9605-6337

https://doi.org/10.1016/j.tox.2022.153371
Received 19 August 2022; Received in revised form 20 October 2022; Accepted 2 November 2022
Available online 14 November 2022

endoplasmic reticulum stress. This study demonstrates novel genes and pathways involved in TCE-induced placental injury and showed antioxidant co-treatment largely did not attenuate TCE exposure effects.

1. Introduction

Volatile organic hydrocarbons are a class of anthropogenic compounds used in a variety of applications harnessing their potent solvent properties. Trichloroethylene (TCE), one of the most commonly utilized hydrocarbons, is used in refrigerant manufacturing and industrial metal degreasing (Chiu et al., 2013). Widespread decades-long usage and improper disposal methods have led to pervasive TCE contamination in the environment despite mitigation (Chiu et al., 2013; Waters et al., 1977). Today, TCE soil, water and air pollution persist in thousands of hazardous sites in the United States and around the world (U.S. EPA (Environmental Protection Agency) 2019a, b). Due to ongoing contamination, residential risk of human TCE exposure remains high.

Pregnant women and their fetuses may be particularly vulnerable to deleterious effects of TCE exposure. Maternal TCE exposure during pregnancy was associated with an elevated risk of fetal growth restriction in several recent epidemiology studies (Forand et al., 2012; Ruckart et al., 2014). Consistent with epidemiological evidence, we previously reported that timed-pregnant Wistar rats exposed to TCE during mid-gestation had decreased fetal weights and elevated oxidative stress biomarkers (Loch-Caruso et al., 2019). In a follow-up study, we co-exposed pregnant Wistar rats to TCE and N-acetylcysteine (NAC), an antioxidant that readily crosses the placenta (Horowitz et al., 1997; Rushworth and Megson, 2014), to investigate mechanistic attenuation of TCE effects by NAC. Our follow-up study confirmed our previous finding of reduced fetal weights, and added an analysis of sex-specific effects, reporting that reduced fetal weight was male-specific (Su et al., 2021). Moreover, TCE co-exposure with NAC (TCE+NAC) reduced fetal weight in both males and females, suggesting TCE+NAC may exacerbate rather than attenuate TCE-induced effects (Su et al., 2021).

To further understand the little-known toxicological mechanisms underpinning TCE- and TCE+NAC-induced decrease in fetal weights, in the current study we investigated changes in gene expression and associated pathway enrichment in the rat placentae, an organ that plays a critical role in regulating fetal growth and physiology. The placenta, the organ that performs essential biological functions for a fetus during development, is a plausible target organ for TCE toxicity because of its high blood perfusion rate and ability to metabolize parent compounds into reactive metabolites (Burton and Fowden, 2015; Elkin et al., 2020). Circulating TCE and its major metabolites cross the placenta and are therefore, in direct contact with placental tissue in vivo (Ghantous et al., 1986; Laham, 1970). Based on the effects of TCE and TCE+NAC effects on fetal weights, we hypothesized that: 1) maternal exposure to TCE would have an adverse albeit sexually-dimorphic impact on gene expression and on pathways associated with cellular function of major organelles such as endoplasmic reticulum and mitochondria and that 2) NAC co-exposure would exacerbate these effects. The focus on these organelles was based on our previous evidence in a placental cell line of TCE metabolite-induced endoplasmic reticulum stress (Elkin et al., 2021) and mitochondria dysfunction (Elkin et al., 2019).

2. Materials and methods

2.1. Experimental design

The overall experimental design is outlined in Fig. 1. The study utilized archived placental samples from our previous study (Su et al., 2021) that investigated the impact of gestational TCE and NAC exposure on fetal outcomes. All procedures with the rats were approved by the University of Michigan Institutional Animal Care & Use Committee (IACUC) (Approval #PRO00006981) and performed in accordance with all state and federal regulations for use of vertebrate animals. Twenty-four timed-pregnant Wistar rats were delivered in 6 batches (4 per batch) for a total of N = 6 (dams)/treatment group. Within each batch, one rat was assigned randomly to each of four treatment groups: control, TCE, TCE+NAC, or NAC, totaling 24 pregnant dams. After the exposure period and subsequent tissue collection, RNA was extracted from one male and one female placenta from each dam. Exposure-induced differential gene expression was measured with RNA-seq and validated with PCR. Pathway enrichment analysis was performed based on differential gene expression results. Differential gene expression analyses were stratified by sex.

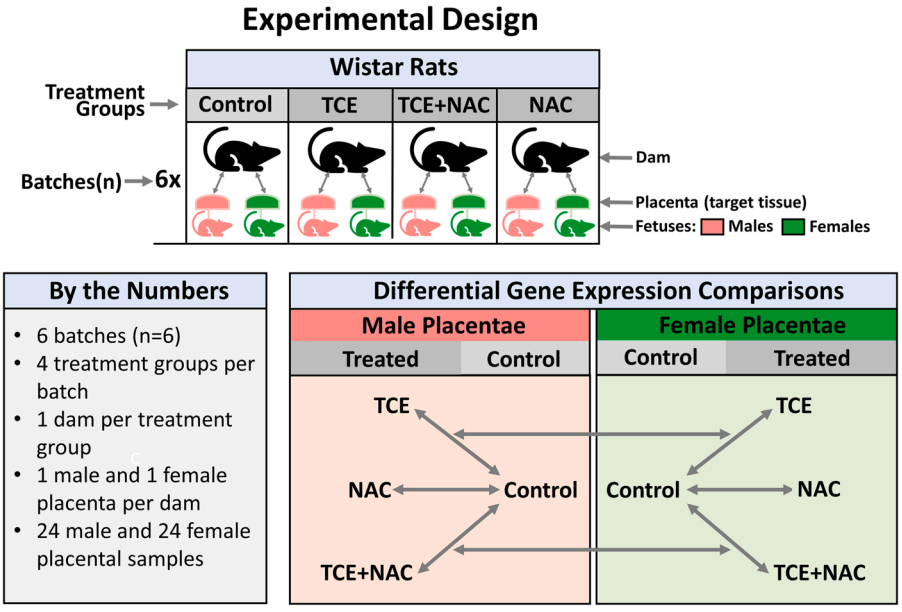

Fig. 1. Overall experimental design. Timed-pregnant Wistar rats were exposed to vehicle control, TCE alone, TCE+NAC, or NAC alone. Exposure-induced differential gene expression was measured with RNA-seq and validated with PCR. Pathway enrichment analysis was performed based on differential gene expression results. Differential gene expression was stratified by sex for analysis. The following treatment comparisons were made for male and female placental tissue: control vs. TCE, control vs. TCE+NAC, and control vs. NAC. N = 6 dams for each treatment group. One male and one female placenta from each dam was used in the differential gene expression analysis. The number of mitochondria in placental tissue was also measured as a follow up to differential gene expression results.

2.2. Chemicals and reagents

Trichloroethylene (TCE) was purchased from Sigma-Aldrich (St. Louis, MO, USA). N-acetyl-L-cysteine (NAC) was obtained from the University of Michigan Hospital pharmacy (pharmaceutical grade).

2.3. Timed-pregnant Wistar rats

Timed-pregnant female Wistar rats (Wistar IGS Rat, Strain Code 003) aged 60–90 days were purchased from Charles River Laboratories (Wilmington, MA, USA). The animals were shipped to the University of Michigan School of Public Health animal facility on gestation day (GD) 2 (day of copulation designated as GD 0). Rats were individually housed in a 12-hour light/dark cycle-controlled environment and fed standard rat chow (Purina 5001) and water ad libitum. On GD 3, the rat weights ranged from 121 to 224 g. Rats in particular were used for this study because they share key placental development characteristics with humans (hemochorial placentation, intrauterine trophoblast invasion and spiral artery remodeling) (Soares et al., 2012), and are the most commonly used economical model for studying pregnancy outcomes in preclinical and pharmaceutical studies (Ain et al., 2006; Grigsby, 2016). Furthermore, studies show that human metabolism of TCE is more similar to metabolism in rats than mice (Lash et al., 2000; Prout et al., 1985). For consistency, the Wistar rat strain was used here because several previous studies which utilized Wistar rats, demonstrated TCE effects on pregnancy-related health outcomes (Healy et al., 1982; Loch-Caruso et al., 2019).

2.4. Chemical exposures

The chemical dosing regimen is summarized in Fig. 2. To minimize stress to the animals, rats were orally exposed to respective chemical treatments via a single mini vanilla wafer cookie (Nabisco; East Hanover, NJ, USA) per rat, as previously described (Seegal et al., 1997). After a 24 h adjustment period post-arrival at the animal facility, rats were given a single mini wafer with no chemicals on GD 3 and GD 4 to train for recognition of the wafer as food. Rats were removed from their regular housing cages and placed individually in empty exposure cages for an hour prior to chemical exposures via wafer cookie. A small hole was carved with a blunt metal tweezers halfway through the width of the wafer to create a small reservoir mid-cookie to hold the chemicals. Chemicals were added directly to the wafers and immediately offered to the rats for consumption. Rats were weighed daily, and chemical treatment doses were prepared according to each rat's individual weight. NAC was dissolved in double-distilled and filtered water prior to pipetting into the wafer reservoir. TCE was pipetted undiluted into the wafer reservoir. The rats typically finished eating the wafer within ten minutes.

2.4.1. Exposure doses

The TCE dose of 480 mg/kg/day was selected because it falls within the mid-range of doses (200–1000 mg/kg TCE) evaluating various biological endpoints in previous rat studies modeling non-inhalation TCE exposures. Several previous studies reported TCE-induced changes: 200 mg/kg-loss of dopaminergic neurons (Liu et al., 2010), 480 mg/kg-decreased fetal weight and increased oxidative stress markers (Loch-Caruso et al., 2019), 1000 mg/kg-nephrotoxicity (Heydari et al., 2017) and neurotoxicity (Liu et al., 2010), while another study using 500 mg/kg reported no toxic effects in fetal heart development (Fisher et al., 2001).

The TCE dose is also within order of magnitude of the U.S. Occupational Safety and Health Administration's permissible inhalation exposure level of 100 parts per million (Agency for Toxic Substances and Disease Registry, 2007). A non-inhalation dose at or above the U.S. OSHA inhalation PEL is justified because inhalation is a more aggressive exposure due to a lack of the first pass effect. As a result, a greater ingestion dosage should be required to produce an equivalent effect (National Research Council US Safe Drinking Water Committee, 1986). Furthermore, various enzymes involved in TCE metabolism are expressed in both rat lung and digestive tract (Yu et al., 2014).

In addition to TCE, 200 mg NAC/kg/day, a chemical with direct and indirect antioxidant properties (Lasram et al., 2015; Shahripour et al., 2014), was given to some rats, either alone or as a co-exposure with TCE. The NAC dose was selected because it falls within a range of doses (100–300 mg/kg NAC) that were previously shown to attenuate oxidative stress effects in rat studies (Chang et al., 2005; Fukami et al., 2004; Naik et al., 2006; Sprong et al., 1998).

2.4.2. Exposure durations

For TCE exposure groups, treatments were administered on GD 6–16. This treatment period was chosen because fetuses and placentae undergo rapid growth and development during this time frame (Furukawa et al. 2011), and are similar to exposure regimens used in previous TCE rat studies (Fisher et al., 1989; Healy et al., 1982; Loch-Caruso et al., 2019). Moreover, this time frame encompasses an observed developmental period of sex-specific differences in rat placental structure, which peak around GD 15 before becoming more similar again by the end of the pregnancy (Kalisch-Smith et al. 2017). For NAC exposure groups, treatments were administered on GD 5–16. NAC exposure on GD 5 was done as a pre-exposure prior to TCE administration to stimulate

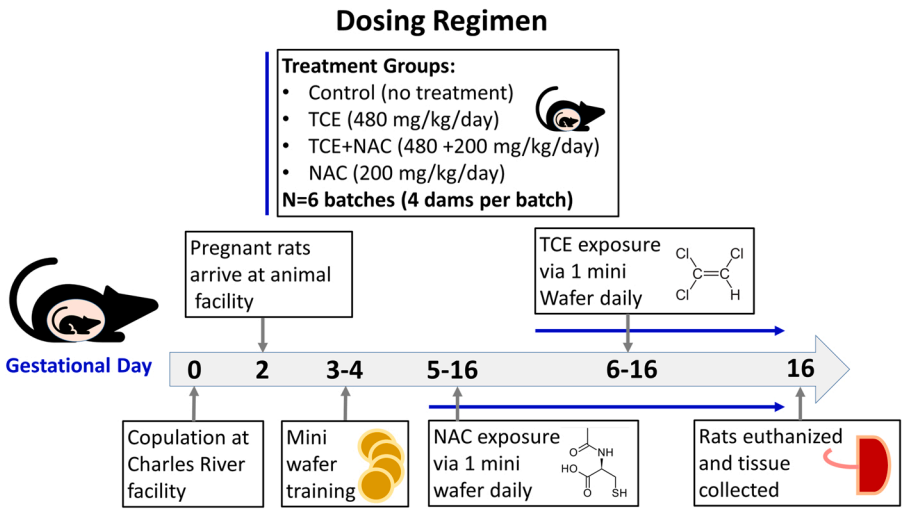

Fig. 2. Dosing Regimen. Following arrival at the animal facility, timed-pregnant Wistar rats were given a single mini vanilla wafer with no chemicals on GD 3 and GD 4 to train for recognition of the wafer as food. Rats were exposed to vehicle control, TCE alone (480 mg/kg/day), TCE+NAC (480 +200 mg/kg/day), or NAC alone (200 mg/kg/day) via vanilla wafer once per day. TCE treatment alone was administered to rats on GD 6–16. For pre-/co-treatment with TCE+NAC, NAC was administered on GD 5–16 and TCE was administered on GD 6–16. NAC treatment alone was administered on GD 5–16. Rats in the vehicle control group received a mini vanilla wafer alone from GD 3–16. Rats were euthanized and tissues collected on GD 16.

transcription of antioxidant genes (Rushworth and Megson, 2014) and increase the chance of TCE effects attenuation. NAC exposure on GD 6–16 was done to match the treatment period chosen for TCE exposure.

2.5. Rat tissue collection

Rats were euthanized on GD 16 by carbon dioxide asphyxiation. Euthanasia was performed directly after completion of wafer treatment on GD 16, and dams were euthanized in random order. Immediately following euthanasia, the uterine horn was removed, placed in a container and kept moist with cold PBS. Intact gestational membranes containing 1 fetus and 1 placenta per sac, were individually dissected out of the uterine horn from left to right. Fetuses were weighed and decapitated via scalpel. Placentae were weighed and laterally dissected to make a subset of placental tissue available for gene expression analysis. Placental tissue for RNA analysis was stored overnight in RNAlater (Qiagen, Hilden, Germany) at 4 °C prior to RNAlater removal and transfer to − 80 °C.

2.6. DNA and RNA isolation

Placenta for and DNA and RNA analysis came from the left side of the uterine horn because placentae were dissected out from left to right. DNA and RNA were extract from randomly a randomly select section of each placenta. RNA was extracted from placental tissue using the RNeasy Plus Mini Kit (Qiagen) following the manufacturer's recommended protocol with a modification. A FastPrep-24 tissue laser (MP Biomedicals; Solon, OH, USA) was utilized prior to the genomic DNA elimination step to achieve maximum quality tissue homogenization. DNA was extracted from placental tissues using the NucleoSpin Tissue kit (Machery-Nagel; Düren, Germany) according to the manufacture's recommended protocol. RNA and DNA concentrations were determined using a NanoDrop 2000 Spectrophotometer (Thermo Fisher Scientific; Waltham, MA, USA). RNA and DNA were subsequently stored at − 80 °C and − 20 °C, respectively, until further processing.

2.7. Fetal sex determination

Fetal sex was determined by the presence (male) or absence (female) of the sex-determining region Y (*Sry*) gene in placental tissue, as determined by qRT-PCR. Fetal sex was confirmed with and concordant for both mRNA and gDNA, as previously described (Su and Loch-Caruso, 2020). Primer sequences used for *SRY* and beta-2 microglobulin (*B2m*) (used as a reference gene) are listed in supplemental Table 1. Reactions and conditions for running and analyzing qRT-PCR are previously described (Su and Loch-Caruso, 2020).

2.8. RNA-sequencing

RNA (6 samples per sex/per group) was transported on dry ice to the University of Michigan Advanced Genomics Core for further processing. RNA concentrations and quality were evaluated using a TapeStation instrument (Agilent; Santa Clara, CA, USA). RIN scores had a mean of 9.7, median of 9.8, minimum of 8.1, and maximum of 10.0. Stranded sequencing libraries for RNA isolated from placental tissue were prepared with the Poly(A) RNA Selection Kit (Lexogen; Vienna, Austria). Libraries were multiplexed (on four lanes) and sequenced using paired-end 300 cycle reads on the NovaSeq 6000 (S4 flow cell) platform (lllumina, San Diego, CA, USA). The range of total number of reads per sample was 13,281,008 to 78,731,529. The average total number of reads per sample was 27,675,544.

2.9. Data processing and quality control

The Great Lakes high-performance computer cluster at the University of Michigan was used for computational analysis. Sequencing read quality was assessed using FastQC (version 0.11.5) (Andrews, 2010). Reports generated for all samples across four lanes were summarized using MultiQC (version 1.8) (Ewels et al., 2016). All mean quality scores were high with phred scores above 35. GC content ranged from 48% to 57%. Between 61.4% and 86% of reads were duplicated. Reads were aligned to a reference rat genome (Rnor_6.0) using STAR (version 2.6.0c) (Dobin et al., 2013), with the options "outFilterMultimapNmax 10" and "sjdbScore 2". Post alignment, QoRTs (version 1.3.6) was used to examine other quality control metrics (Hartley and Mullikin, 2015). Approximately 10–50% of reads per sample were dropped for multi-mapping. Approximately 90% of reads mapped to gene regions. Aligned reads were assigned to Rnor_6.0 genes using featureCounts (version 2.0)(Liao et al., 2014).

Table 1
Endoplasmic reticulum stress-induced Unfolded Protein Response (UPR) transcription factors tested for overrepresentation using hypergeometric testing amongst differentially expressed genes (based on FDR<0.05 criterion). [&]Ampersand denotes significant difference compared to control ($P < 0.05$).

Sex	Treatment Group	Transcription Factor	Pvalue	#Gene Targets	Enriched Gene Targets (DGE: FDR<0.05)
	Control vs. TCE	ATF6	0.0000 **&**	17	*Dnajb11, Dnajc3, Edem1, Ero1b, Hsp90b1, Hyou1, Nol4, Nptx1, Nucb2, Pdia4, Rab2a, Sec23a, Sec24d, Sel1l, Slc30a5, Syvn1, Tfe3*
		ATF4	0.8687	7	*not significant*
		XBP1	0.0380 **&**	7	*Arfgap3, Map3k13, Pdia4, Sec24d, Sec61a1, Slc30a5, Uso1*
Females	**Control vs. TCE+NAC**	ATF6	0.0001 **&**	10	*Arf4, Dnajb11, Dnajc3, Dusp4, Hsp90b1, Nucb2, Pitx2, Rab2a, Slc30a5, Tfe3*
		ATF4	0.1349	15	*not significant*
		XBP1	0.4017	3	*not significant*
	Control vs. NAC	No genes met FDR criterion			
	Control vs. TCE	ATF6	0.0000 **&**	4	*Dnajb11, Hsp90b1, Hyou1, Rab2a*
		ATF4	0.0323 **&**	2	*Hspa5, Wars*
		XPB1	NA	0	*not significant*
Males	**Control vs. TCE+NAC**	ATF6	0.0000 **&**	5	*Dnajb11, Hsp90b1, Hyou1, Orm1, Pdia4*
		ATF4	0.0712	3	*not significant*
		XPB1	0.2159	1	*not significant*
	Control vs. NAC	*No genes met FDR criterion*			

[&]Ampersand denotes significant difference compared to control ($P < 0.05$).

2.10. RNA sequencing data analysis

Rat placenta samples were analyzed for differential gene expression in R statistical software (version 4.0.2) with the DESeq2 package (version 1.24.0) (Love et al., 2014). Genes with mean read counts-per-million less than six were filtered out and excluded from the analysis to reduce dispersion due to low expression levels. After filtering,

16,661 genes were included in the analyses. Data were normalized using the median of ratios method (Anders and Huber, 2010). To remove random variation, RUV (Remove Unwanted Variation) normalization factors were generated for each sample using the RUVSeq package (Risso et al., 2014). Principal components analysis (PCA) was performed, calculated based on variance of log-transformed expression data of the top 500 genes. Principal components were plotted to examine clustering on relevant covariates, including treatment, sex, batch and dam. Student's t-test (for two groups) or one-way ANOVA (for three or more groups) were used to test for associations between covariates and PCA dimension 1 or 2. Negative binomial general linear modeling was used for differential gene expression testing. Samples were stratified by sex and analyzed separately. The following comparisons for males or females were made between respective treatment groups: control vs. TCE, control vs. TCE+NAC, and control vs. NAC. Models were adjusted for batch, dam, and RUV normalization factor. Genes were considered differentially expressed between non-treated and treated samples with an adjusted p-value < 0.05 using the Benjamini-Hochberg false discovery rate (FDR) method (Benjamini and Hochberg, 1995). Treatment -induced upregulation $>$ 2-fold or downregulation < -2-fold are denoted throughout the results section. These fold-change values equate to $\log_2$ fold-change (logFC) > 1 (upregulation) or < -1 (downregulation).

2.11. Pathway enrichment analyses

To identify biological pathways and processes impacted by TCE, NAC or TCE+NAC treatment, pathway enrichment analyses were performed using RNA-Enrich, a new analysis option offered on the LR Path website. The RNA-enrich option uses logistic regression on continuous expression data to test for gene set enrichment amongst pathways (Lee et al., 2016; Sartor et al., 2009). RNA-Enrich does not require a significance cutoff for genes included in the analyses nor gene count cutoffs, however, 4378 uncharacterized and/or unannotated genes were excluded, leaving 12, 172 genes included in the analysis. The following were also included in the analysis: FDR, $\log_2$fold-change, directionality, and average read count for each gene test. Tests were run for Gene Ontology Biological Process pathways and enriched transcription factors. An enrichment odds ratio and FDR were calculated for each enriched pathway. Because of the large number of enriched pathways, pathways representing with an FDR < 0.01 were considered significantly enriched, rather than the standard FDR< 0.05. Enrichment odds ratios < 1 indicated downregulation, and enrichment odds ratios > 1 indicated upregulation of pathway represented by gene set. Enriched pathways were further screened for redundancy with REVIGO, a webtool designed to summarize and remove redundant gene ontology terms, with the following options: medium (0.7) allowed similarity and SimRel semantic similarity measure (Supek et al., 2011).

2.12. Enrichment testing of transcription factor gene targets

Because endoplasmic reticulum stress was a key enriched pathway, gene targets of the ATF4, ATF6, and XBP1 unfolded protein response transcription factors were tested for overrepresentation among differentially expressed genes based on differential gene expression results. ATF6 gene targets were identified from TRANSFAC, a curated database of transcription factors and target genes based on transcription factor binding site predictions (Matys et al., 2003; Matys et al., 2006) and Adachi et al. (2008). Empirically determined ATF4 gene targets were identified from mouse embryo fibroblasts ChIP-seq analysis (Han et al., 2013). Two additional ATF4 gene targets, *Pmaip1* and *Psph*, were also included (Sharma et al., 2018; Yang et al., 2018; Zhao et al., 2014). XBP1 gene sets were identified from TRANSFAC (Matys et al., 2003; Matys et al., 2006). Genes regulated by ATF4 (N = 383), ATF6 (N = 115) and XBP1 (N = 132) were tested for enrichment in TCE-exposed and TCE+NAC-exposed genes with differential expression meeting FDR< 0.05 criterion. Target gene enrichment tests were performed using the phyper function (hypergeometric test) (R Core Team, 2019).

2.13. Real-time quantitative PCR (qRT-PCR) validation

Relevant differentially expressed genes measured by RNA-seq were validated using qRT-PCR. These genes included: *Atf4*, *Atf6*, *Ddit3* (CHOP), *Il17*, *Sirt3*, *Trb3*. Primary sequences, shown in supplemental Table 1, were obtained from Chen et al. (2014) (*Trb3, Ddit3,* and *Atf4*), Loof et al. (2016) (*Il17* and *Actb*), (*Atf6*), and Luo et al. (2017) (*Sirt3*). The qRT-PCR was performed on the same respective male and female rat placentas (Control, TCE, TCE+NAC) used for RNA-seq. The qRT-PCR reactions were prepared with SYBR Green Mastermix (SABiosciences) and custom synthesized primers (Integrated DNA Technologies; Coralville, IA), and run on a Bio-Rad (Hercules, CA) CFX96 Real Time C1000 thermal cycler following the manufacturer's recommended protocols. The mRNA levels of each gene of interest were normalized to β-actin (*Actb*) mRNA levels. The gene expression levels were calculated using the $2^{-\Delta\Delta CT}$ Method (Livak and Schmittgen, 2001) and displayed as fold-change levels compared to controls.

2.14. Measurement of mitochondrial DNA content

Relative mitochondrial DNA content, a proxy for mitochondrial copy number, was estimated by calculating the ratio of mitochondrial DNA to nuclear DNA (*Actb),* as measured by qRT-PCR. Following DNA extraction, qRT-PCR was performed on genomic DNA from rat placenta using a commercially available Rat Mitochondrial DNA Copy Number Kit (Detroit R&D; Detroit, MI, USA) containing primers for one nuclear encoded gene; *Actb* and a mitochondrial encoded gene. Primers sequences are proprietary and not given in the kit. Real-time PCR reactions were prepared with primers and SYBR GreenMastermix (Qiagen SABiosciences; Sioux Falls, SD, USA), and run on a Bio-Rad (Hercules, CA) CFX96 Real Time C1000 thermal cycler following the manufacturer's recommended protocols. The mitochondrial content was calculated using a calculation tool developed by Takara Bio, Inc. (Takara, 2013a). Briefly, the difference in the Ct values (ΔCt) for the mtDNA */Actb* pair was calculated, followed by calculation of 2ˆ-(ΔCt). Mitochondrial DNA content was measured in one male and one female placenta from each dam in each respective treatment group (controls, TCE, TCE+NAC) and analyzed with one-way analysis of variance (ANOVA), followed by Tukey's or Dunnett's post-hoc test for comparison of means using GraphPad Prism software (GraphPad Software Inc; San Diego, CA, USA). A p-value< 0.05 was considered statically significant.

3. Results

3.1. Overall summary of exposure induced differential gene expression

In PCA diagrams depicting all 48 samples plotted on relevant covariates, no specific clustering patterns were observed (Supp. Fig. 1). Only one covariate, dam, was associated with PCA dimension 2 (P = 0.01), and none were associated with PCA dimension 1. All samples were subsequently stratified by sex and analyzed for differential gene expression and pathway enrichment between controls and respective treatment groups. A heatmap depicting expression levels for the 40 genes with the largest magnitude fold-change (up and downregulated) for each treated versus control comparison, organized by hierarchical clustering, is shown in Fig. 3. The following treatment comparisons were made for female and male placentae, respectively: control vs. TCE, control vs. TCE+NAC, and control vs. NAC. For reference purposes, comparisons were also made for male and female placenta for the NAC vs. TCE+NAC treatment groups (Supp. Fig. 2).

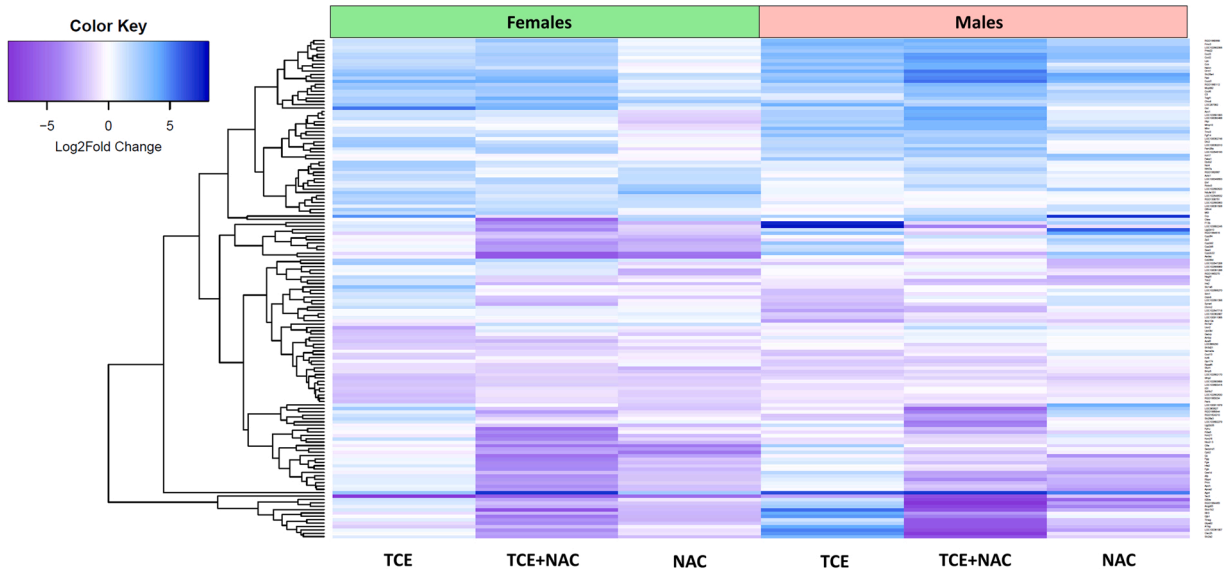

Fig. 3. Top log_2fold-change gene expression levels for comparisons between various treatment groups and control placental samples stratified by sex. Heatmap depicts expression levels for the 25 genes with the largest magnitude log_2fold-change (up and downregulated) from each of the following comparisons: control vs. TCE, control vs. TCE+NAC, and control vs. NAC.

3.2. Summary of exposure induced differential gene expression in female placental tissues

In female placental tissues, maternal exposure to both TCE alone and TCE+NAC altered the gene expression levels of hundreds of genes with minimal overlap between female exposure groups, compared to control tissues. For example, only 14 differentially expressed genes overlapped between groups, whereas over one hundred genes were uniquely differentially expressed in each respective group (Fig. 4A, FDR<0.05 + FC>2). TCE-exposed tissues had 350 differentially expressed genes that met the FDR < 0.05 criterion only, 598 genes with a fold-change magnitude difference > 2 only, and 129 genes that met both criteria (114 upregulated and 15 downregulated) (Fig. 4B, Suppl. Table 2). Likewise, TCE co-exposure with NAC (TCE+NAC) yielded similar results with 388 differentially expressed genes that met the FDR < 0.05 criterion only, 669 genes with a fold-change magnitude difference > 2 only, and 125 genes that met both criteria (55 upregulated and 70 downregulated) (Fig. 4C, Suppl. Table 3). Unlike the TCE and TCE+NAC treatment groups, NAC exposure alone did not yield any differentially expressed genes that met the FDR < 0.05 criterion; however, 496 genes had a fold-change magnitude difference > 2 (Fig. 4D, Suppl. Table 4). Differentially expressed genes with the smallest FDR criterion in the female treatment groups compared to controls included: *Slc17a5* upregulated 1.9-fold (FDR=1.1×10^{-11}) in the TCE group, *LOC100912380* downregulated 2.9-fold (FDR=5.3×10^{-12}) in the TCE+NAC group, and *Sgms2* downregulated 1.7-fold (FDR=0.06) in NAC group.

To further evaluate how TCE co-exposure with NAC modified differential gene expression compared to TCE alone or NAC alone, correlations of effect estimate across different female treatment groups were evaluated. Changes in female gene expression relative to control were more strongly correlated for tissues exposed to TCE+NAC versus NAC alone [$r = 0.64$, $P < 1.0 \times 10^{-15}$] (Fig. F) than TCE+NAC versus TCE alone [$r = 0.44$, $P < 1.0 \times 10^{-15}$] (Fig. 4E). Because the TCE+NAC versus NAC alone correlation coefficient was higher than the TCE+NAC versus TCE alone correlation coefficient, these findings suggest that NAC contributed more than TCE to the extent of differential gene expression in TCE+NAC treatment group compared to controls. This resulted in an altered gene expression profile for the co-exposure that more closely matched that of NAC than that of TCE.

3.3. Summary of exposure induced enriched pathways in female placental tissues

Genes with altered placental expression levels in female TCE, TCE+NAC, and NAC exposure groups were enriched in numerous biological pathways (Fig. 5A &B, Suppl. Tables 8, 9 & 10). The TCE group had 43 enriched pathways (FDR<0.01), the TCE+NAC group had 88 enriched pathways (FDR<0.01), and the NAC group had 494 enriched pathways (FDR<0.01). When clustering enriched pathways into biological categories, the category distribution for the TCE+NAC group more closely matched the NAC group than the TCE group, consistent with correlation patterns of gene expression. In the female TCE+NAC and NAC groups, the largest single category was tissue development (TCE+NAC: 38% of enriched pathways & NAC: 31% of enriched pathways) which included numerous downregulated pathways, such as 'anatomical structure development' (TCE+NAC: enriched odds ratio=0.9, FDR=3.8×10^{-3}) (NAC: enriched odds ratio=0.7, FDR=9.3×10^{-28}). In contrast, the largest category in the TCE group was subcellular processes (30% of enriched pathways), which included downregulated mitochondrial-related pathways such as 'cellular respiration' (enriched odds ratio=0.7, FDR=3×10^{-3}) and upregulated endoplasmic reticulum-related pathways, such as 'response to endoplasmic reticulum stress' (enriched odds ratio=1.4, FDR=2.6×10^{-5}). Interestingly, 'response to endoplasmic reticulum stress' was also enriched by TCE+NAC (enriched odds=1.7, FDR=1.3×10^{-9}) and NAC (enriched odds ratio=2.3, FDR=2.4×10^{-11}). Notable differences between pathways enriched by the female exposure groups were observed in the immune response category. TCE+NAC downregulated 'gamma-delta T cell activation' (enriched odds ratio=0.3, FDR=6.0×10^{-4}) and upregulated 'chronic inflammatory response' (enriched odds ratio=2.2, FDR=5.6×10^{-5}), whereas NAC only downregulated 'inflammatory response' (enriched odds ratio=0.8, FDR=2.7×10^{-3}). Moreover, this category was absent altogether from TCE group. Together, these results highlight key similarities and differences in the pathways enriched by the female treatment groups.

3.4. Summary of exposure induced differential gene expression of male placental tissues

Distinctive from female placental tissues, in male placental tissues,

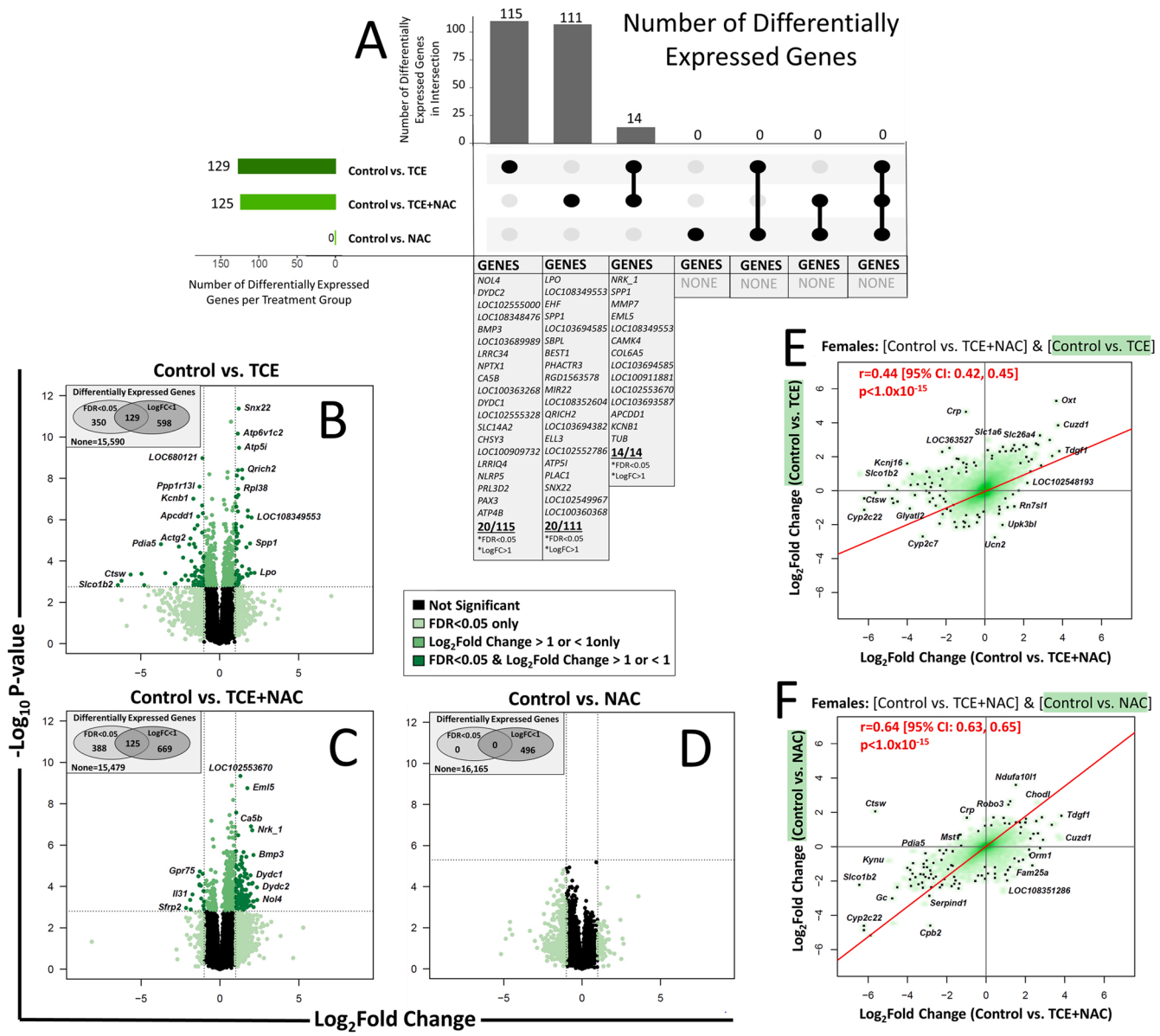

Fig. 4. Exposure-induced differential gene expression of female placental tissues. Differential gene expression in female placental tissue was evaluated for the following treatment comparisons: control vs. TCE, control vs. TCE+NAC, and control vs NAC. Differential gene expression was analyzed using the DESeq2 package for R using negative binomial general linear modeling with RUV and batch correction. N = 6 independent experiments. A) Upset plot depicting number and overlap of differentially expressed genes between comparisons of controls vs. TCE, TCE+NAC, or NAC. FDR < 0.05 + $\log_2$fold-change > 1 [fold-change > 2] were considered differentially expressed. Volcano plots comparing differential gene expression between controls and: B) TCE, C) TCE+NAC, or D) NAC. Genes fulfilling the following criteria are denoted by color: FDR < 0.05 only (light green), $\log_2$fold-change magnitude > 1 [fold-change > 2] only (forest green), and FDR < 0.05 + $\log_2$fold-change magnitude > 1 [fold-change > 2] (dark green). Numbers of differential expressed genes by criterion (FDR and/or fold-change) are shown in Venn diagram insets. Plots depicting correlation of $\log_2$fold-change in gene expression between: E) [control vs TCE+NAC] and F) [control vs. TCE] or [control vs. TCE+NAC] and [control vs. NAC]. Pearson's correlation coefficients (r) were calculated for the pairwise comparison of logFC values for all dually expressed genes between respective comparisons. Pathway enrichment analyses were performed using RNA-Enrich for GOBP gene sets. Gene sets representing with an FDR< 0.01 were considered significantly enriched.

maternal exposure to TCE alone and TCE+NAC altered the gene expression levels of only a small number of genes with substantial overlap, compared to control tissues. For example, 4 genes were differentially expressed (FDR<0.05 + fold-change >2) in common with both treatment groups, while only 5 or 30 differentially expressed genes were unique to the TCE alone and TCE+NAC treatment groups, respectively (Fig. 6A). Summarizing altered gene expression for individual treatment groups, TCE-exposed tissues had 21 differentially expressed genes that met FDR< 0.05 criterion only, 504 genes with a fold-change magnitude difference > 2 only, and 9 genes that met both criteria (7 upregulated and 2 downregulated) (Fig. 6B, Suppl. Table 5). Moreover, co-exposure with TCE+NAC yielded 33 differentially expressed genes that met FDR< 0.05 criterion only, 654 genes with a fold-change magnitude difference > 2 only, and 35 genes that met both criteria (26 upregulated and 4 downregulated (Fig. 6C, Suppl. Table 6). NAC exposure alone did not yield any differentially expressed genes that met FDR< 0.05 criterion; however, 441 genes had fold-change magnitude difference > 2 only (Fig. 6D, Suppl. Table 7). Differentially expressed genes with the smallest FDR criterion in the male treatment groups compared to control included: *Sil1* upregulated 1.5-fold (FDR=7.8 $\times 10^{-8}$) in the TCE group, *Cyp2c7* downregulated 29.9-fold (FDR=1.4 $\times 10^{-8}$) in the TCE+NAC group, and *Serp1* downregulated

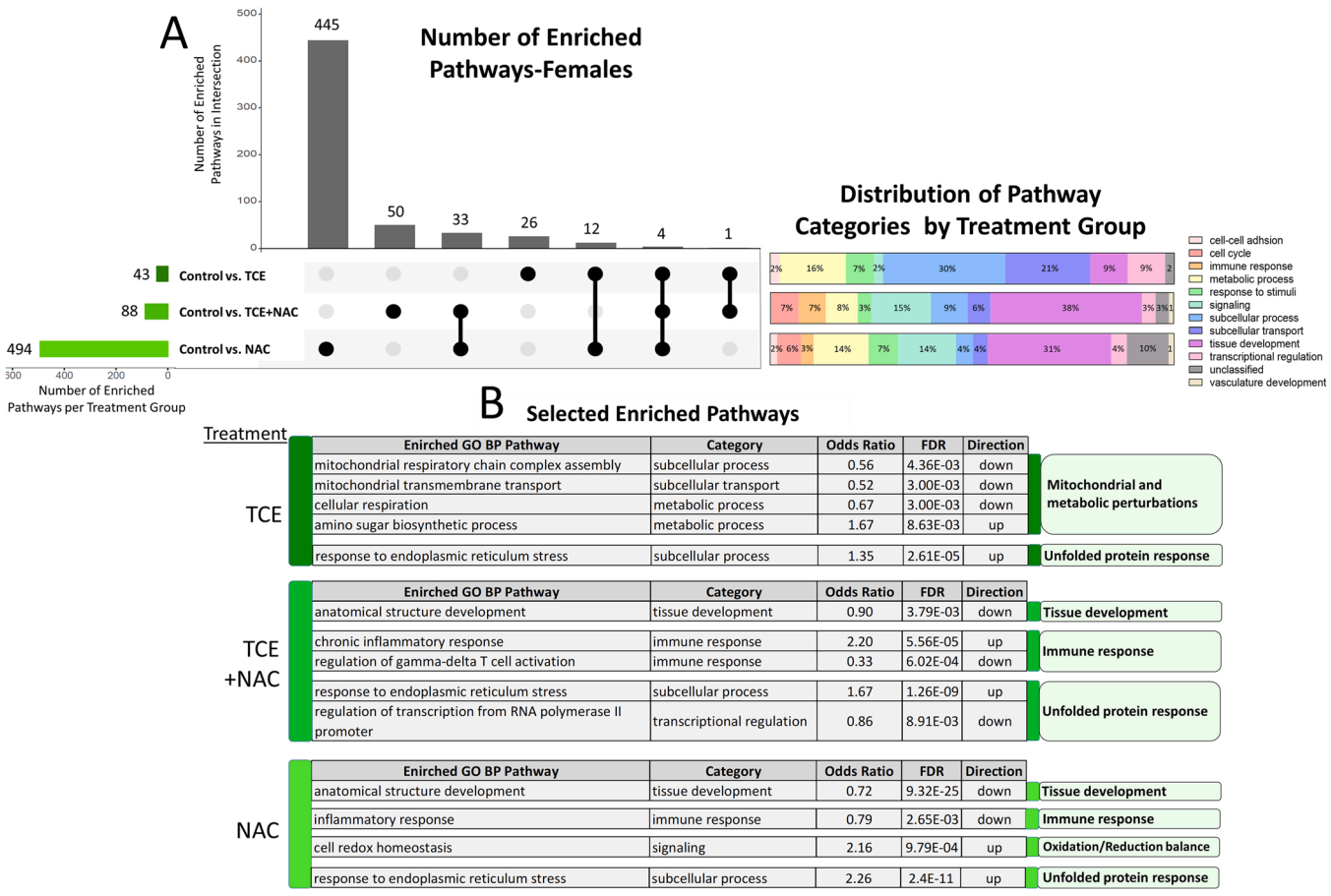

Fig. 5. Exposure-induced enriched pathways of female placental tissues. A) Upset plot depicting number and overlap of enriched pathways between comparisons of controls vs. TCE, TCE+NAC, or NAC, and ribbon depicting distribution of enriched pathways categorized by biological function. B) Selected up and downregulated enriched pathways categorized by biological function for each treatment comparison. Enriched odds ratio, FDR and direction of change are shown.

1.3-fold (FDR=0.05) in NAC group.

To evaluate how TCE co-exposure with NAC modified differential gene expression in males compared to TCE alone or NAC alone, correlations of effect estimate across different male treatment groups were evaluated. Changes in gene expression relative to control were similarly correlated for tissues exposed to TCE+NAC versus TCE alone [$r = 0.39$, $P < 1.0 \times 10^{-15}$] (Fig. 6E) and TCE+NAC versus NAC alone [$r = 0.37$, $P < 1.0 \times 10^{-15}$] (Fig. 6 F). Because the correlation coefficients are very similar, these findings suggest that both TCE and NAC contribute equally to the extent of differential gene expression in the TCE+NAC treatment group compared to controls, resulting in an altered gene expression profile for the co-exposure that equally resembled that of NAC alone and TCE alone.

3.5. Summary of exposure induced enriched pathways in male placental tissues

Like females, the male treatment groups also had numerous genes with altered expression enriched (FDR<0.01) in biological pathways (Fig. 7A & 7B, Suppl. Tables 11, 12 & 13). The TCE group had 88 enriched pathways, the TCE+NAC group had 101 enriched pathways, and the NAC group had 185 enriched pathways. Consistent with correlation patterns of gene expression, the biological category distribution for all three treatment groups was relatively similar. In all groups, the largest category was tissue development (TCE: 27% of enriched pathways, TCE+NAC: 37% of enriched pathways, and NAC: 30% of enriched pathways) which included downregulated pathways, such as 'morphogenesis of an endothelium' (TCE: enriched odds ratio=0.4, FDR=5.6×10^{-3}) (TCE+NAC: enriched odds ratio=0.4, FDR=4.5×10^{-4}) (NAC: enriched odds ratio=0.4, FDR=1.5×10^{-3}). Moreover, upregulated 'response to endoplasmic reticulum stress'- in the subcellular process category- was also enriched in all groups (TCE: enriched odds ratio=1.8, FDR=1.8×10^{-11}) (TCE+NAC: enriched odds ratio=1.7, FDR=1.3×10^{-9}) (NAC: enriched odds ratio=2.2, FDR=3.4×10^{-17}). In the immune response category, exposure groups had both similarities and differences between enriched pathways. Downregulated 'gamma-delta T cell activation' was enriched in the TCE and TCE+NAC groups (TCE: enriched odds ratio=0.3, FDR=3.6×10^{-4}) (TCE+NAC: enriched odds ratio=0.4, FDR=0.02), while the TCE+NAC group had additional pathways enriched for a pro-inflammatory response such as 'chronic inflammatory response' (enriched odds ratio=2.2, FDR=1.2×10^{-5}). Furthermore, the immune system category was absent from NAC group. Distinctive from the TCE and NAC groups, the TCE+NAC group also had several notable enriched signaling pathway including 'insulin-like growth factor receptor signaling' (enriched odds ratio=0.4, FDR=8.7×10^{-4}) and 'RAS protein signal transduction' (enriched odds ratio=0.7, FDR=9×10^{-3}). These results underscore important similarities and differences enriched by the male treatment groups.

3.6. Exposure induced differential gene expression in male versus female placental tissues

To further understand sex-related gene expression changes from TCE exposure to placental tissues compared to controls, several direct comparisons were made between differential gene expression in TCE-treated

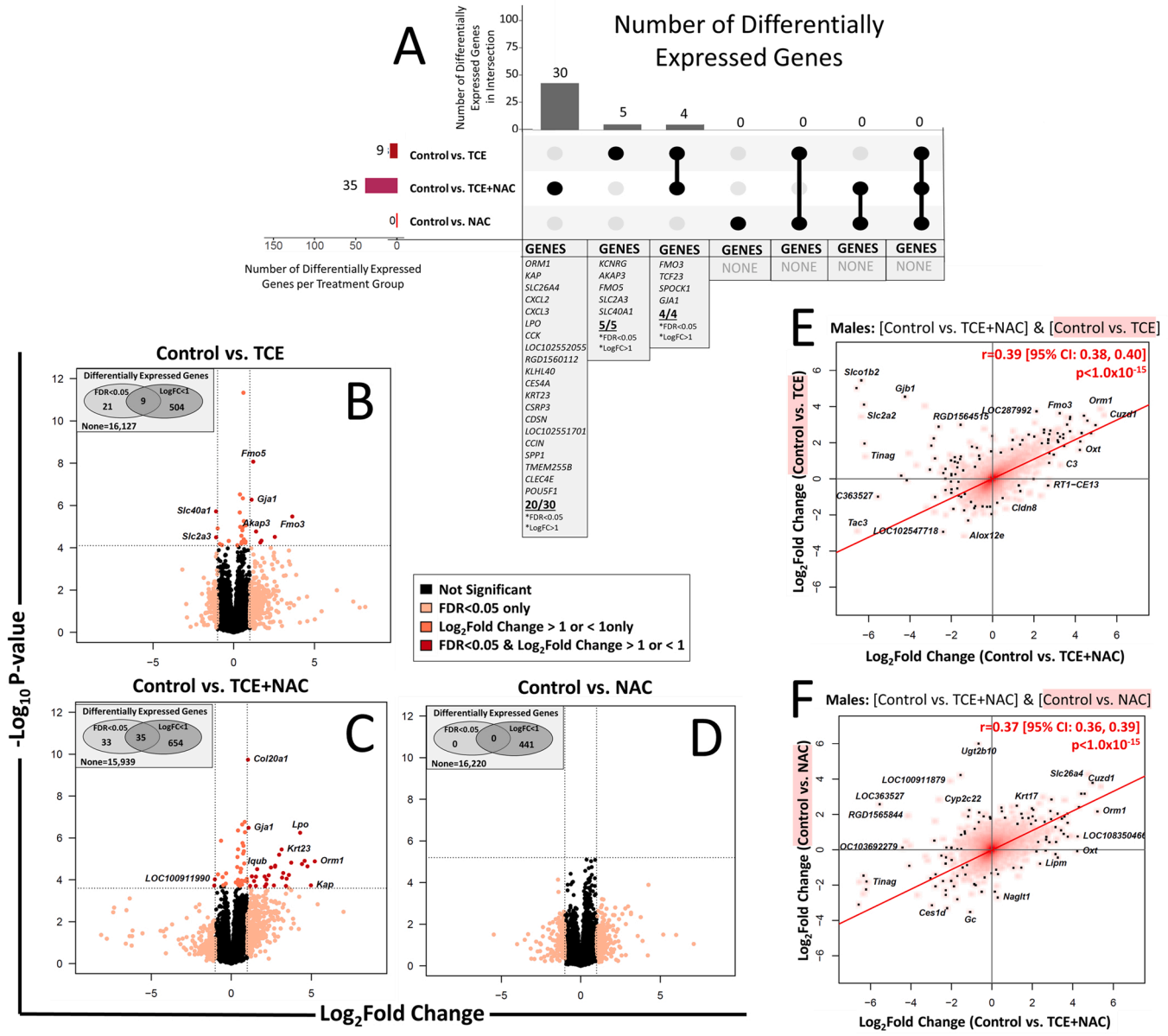

Fig. 6. Exposure-induced differential gene expression of male placental tissues. Differential gene expression in male placental tissue was evaluated for the following treatment comparisons: control vs. TCE, control vs. TCE+NAC, and control vs NAC. Differential gene expression was analyzed using the DESeq2 package for R using negative binomial general linear modeling with RUV and batch correction. N = 6 independent experiments. A) Upset plot depicting number and overlap of differentially expressed genes between comparisons of controls vs. TCE, TCE+NAC or NAC. FDR < 0.05 + log_2fold-change > 1 [fold-change > 2]) were considered differentially expressed. B) Volcano plots comparing differential gene expression between controls and: B) TCE, C) TCE+NAC, or D) NAC. Genes fulfilling the following criteria are denoted by color: FDR < 0.05 only (salmon), log_2fold-change magnitude > 1 [fold-change > 2] only (orange), and FDR < 0.05 + log_2fold-change magnitude > 1 [fold-change > 2] (red). Plots depicting correlation of logFC in gene expression between: E) [control vs TCE+NAC] and F) [control vs. TCE] or [control vs. TCE+NAC] and [control vs. NAC]. Numbers of differential expressed genes by criterion (FDR and/or log_2fold-change) are shown in Venn diagram insets. Pearson's correlation coefficients (r) were calculated for the pairwise comparison of log_2fold-change values for all dually expressed genes between respective comparisons. Pathway enrichment analyses were performed using RNA-Enrich for GOBP gene sets. Gene sets representing with an FDR< 0.01 were considered significantly enriched.

and TCE+NAC-treated male and female placental tissues. Of the differentially expressed genes that met both FDR and fold-change criteria (FDR<0.05 + fold-change >2), only one gene, *Fmo5*, was differentially expressed in the TCE groups compared to controls in both sexes (Fig. 8A). Moreover, TCE+NAC exposure in both males and females significantly altered gene expression of three genes compared to controls: *Kcnb1, Lpo* and *Spp1* (FDR<0.05 + fold-change >2]) (Fig. 8B). Correlations of expression levels across male and female treatment groups were also evaluated. Changes in gene expression relative to control were equally correlated for tissues exposed to TCE+NAC-males versus TCE+NAC-females [$r = 0.56$, $P < 1.0 \times 10^{-15}$] (Fig. 8C) and TCE-males versus TCE-females [$r = 0.50$, $P < 1.0 \times 10^{-15}$] (Fig. 8D).

3.7. Evidence of exposure induced endoplasmic reticulum stress across male and female placental tissue

Consistent with strong correlation of gene expression between males and females, there were several pathways that were enriched across multiple treatment groups in both sexes. One of these pathways, upregulated 'response to endoplasmic reticulum stress,' was the only

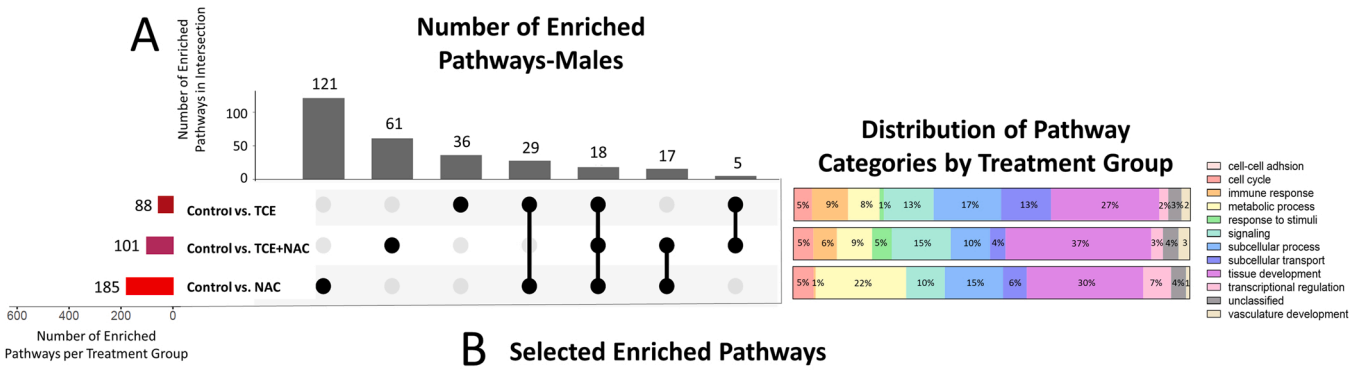

B Selected Enriched Pathways

Treatment	Enirched GO BP Pathway	Odds Ratio	FDR	Direction	
TCE	morphogenesis of an endothelium	0.39	0.0056	down	Tissue development
	gamma-delta T cell activation	0.30	0.0004	down	Immune response
	response to endoplasmic reticulum stress	1.79	0.0000	up	Unfolded protein response
	regulation of transcription from RNA polymerase II promoter	0.84	0.0039	down	
TCE +NAC	morphogenesis of an endothelium	0.38	0.0004	down	Tissue development
	gamma-delta T cell activation	0.41	0.0200	down	Immune response
	B cell activation	0.60	0.0002	down	
	chronic inflammatory response	2.21	0.0000	up	
	chemokine-mediated signaling pathway	1.81	0.0004	up	
	response to progesterone	1.61	0.0086	up	Signaling
	insulin-like growth factor receptor signaling pathwa	0.43	0.0009	down	
	positive regulation of TOR signaling	1.84	0.0053	up	
	Ras protein signal transduction	0.73	0.0090	down	
	response to endoplasmic reticulum stress	1.67	0.0000	up	Unfolded protein response
	negative regulation of transcription from RNA polymerase II promoter	0.80	0.0063	down	
NAC	morphogenesis of an endothelium	0.36	0.0015	down	Tissue development
	cell redox homeostasis	1.91	0.0007	up	Oxidation/Reduction balance
	response to endoplasmic reticulum stress	2.15	0.0000	up	Unfolded protein response
	regulation of transcription from RNA polymerase II promoter	0.78	0.0000	down	

Fig. 7. Exposure-induced enriched pathways of male placental tissues. A) Upset plot depicting number and overlap of enriched pathways between comparisons of controls vs. TCE, TCE+NAC, or NAC, and ribbon depicting distribution of enriched pathways categorized by biological function. B) Selected up and downregulated enriched pathways categorized by biological function for each treatment comparison. Enriched odds ratio, FDR and direction of change are shown.

pathway enriched across all groups. Endoplasmic reticulum stress in cells activates the unfolded protein response (UPR), a condition intended to refold or degrade accumulated misfolded proteins in the endoplasmic reticulum. Because the UPR involves specific regulation of transcriptional activity, the gene targets of key UPR transcription factors, ATF4, ATF6, and XBP1 were tested for overrepresentation among differentially expressed genes meeting FDR< 0.05 criterion (Table 1). In the female TCE group, 4% (17 genes) were ATF6 gene targets ($P = 9.9 \times 10^{-8}$) and 1% (7 genes) were XBP1 targets ($P = 0.038$). Likewise, in the female TCE+NAC group, 2% (10 genes) were ATF6 targets ($P = 3.8 \times 10^{-3}$); however, XBP1 targets were not significantly modified. Moreover, female TCE and TCE+NAC groups did not show overrepresentation of ATF4 genes. In the male TCE group, 13% (4 genes) were ATF6 gene targets ($P = 5 \times 10^{-6}$) and 7% (2 genes) were ATF4 targets ($P = 0.032$). Likewise, in the TCE+NAC group, 8% (5 genes) were ATF6 gene targets ($P = 2.5 \times 10^{-5}$); however, ATF4 targets were not significantly modified. Moreover, male TCE and TCE+NAC groups did not have an overrepresentation of XBP1 genes. The male and female NAC groups did not have any differentially expressed genes that met the FDR criterion and were not tested for enrichment.

To further characterize the enriched endoplasmic reticulum stress pathways, 12 UPR genes were clustered by expression patterns using hierarchical clustering and single gene-level logFC were displayed (Fig. 9A). These genes were selected because their differential gene expression met FDR< 0.05 criterion in at least one group (5 genes), they were enriched in the endoplasmic reticulum stress pathway (10 genes) and/or they are key UPR functional genes (4 genes) (Fig. 9B). Five genes had a magnitude fold-change of 0.5 or above in the TCE and TCE+NAC groups for both sexes. Four out of five of these genes were ATF6 gene targets, consistent with the significant overrepresentation results for ATF6 targets in the same groups. These results suggest that the ATF6 branch of the UPR dominates the endoplasmic reticulum response to TCE and/or NAC exposure. Additionally, the *Trib3* gene was specifically upregulated in the male TCE and TCE+NAC groups, albeit not within FDR< 0.05 criterion. Upregulation of this gene is noteworthy because it is a dual gene target of ATF4 and CHOP proteins which dimerizes a largely pro-apoptotic program (Bromati et al., 2011; Han et al., 2013; Ohoka et al., 2005). This result is consistent with ATF4 overrepresentation in the male TCE group and may suggest male-specific activation of the PERK/ATF4-mediated branch of the UPR.

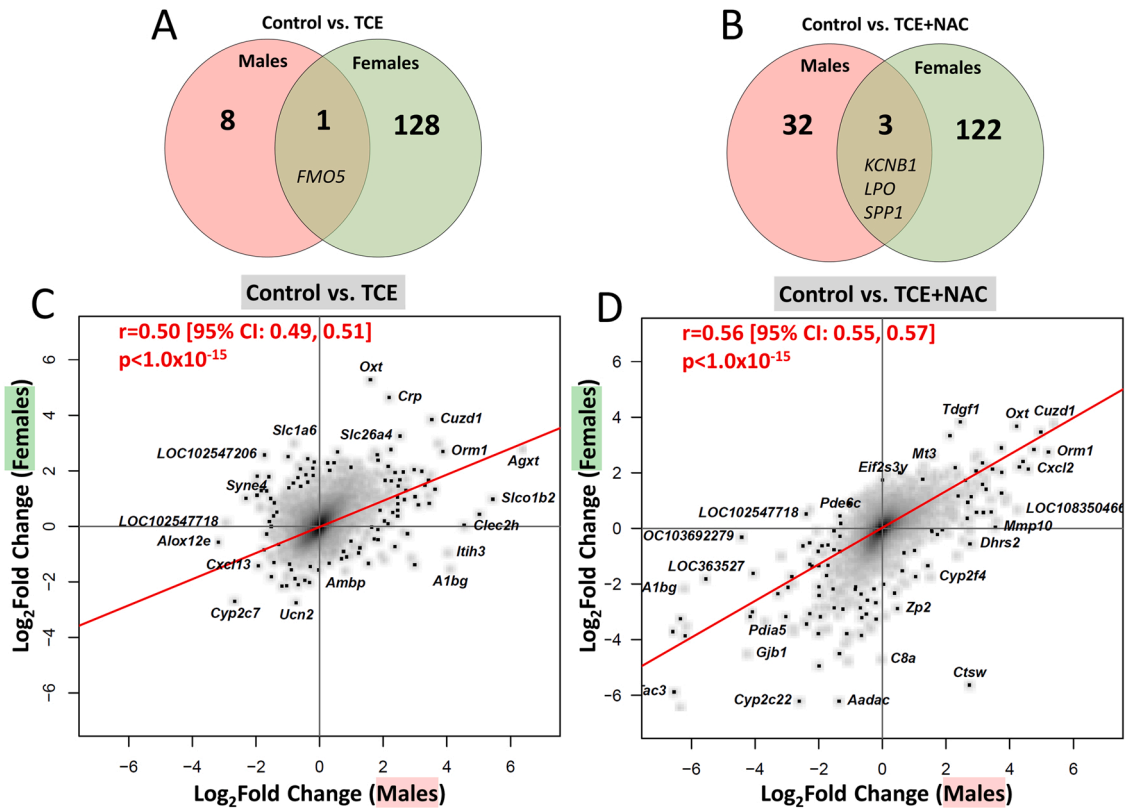

Fig. 8. Exposure-induced differential gene expression in male versus female placental tissues. To further understand sex-related gene expression changes from TCE exposure to placental tissues compared to controls, several direct comparisons were made between differential gene expression in TCE-treated and TCE+NAC-treated male and female placental tissues. Venn diagrams depicting overlap of differentially expressed genes for A) female vs. male TCE groups and B) female vs. male TCE+NAC groups. Plots depicting correlation of log_2fold-change in gene expression between: C) female vs. male TCE groups and D) female vs. male TCE+NAC groups. Pearson's correlation coefficients (r) were calculated for the pairwise comparison of logFC values for all dually expressed genes between respective comparisons.

3.8. Exposure impacts on the gamma delta (γδ) T cell activation pathway across male and female placental tissue

Another noteworthy pathway that was enriched across multiple treatment groups in both sexes was downregulation of γδ T cell activation. This pathway was enriched in the female TCE+NAC group and male TCE and TCE+NAC groups. To characterize the effects of specific regulators on activation of γδ T cells, 10 relevant genes that code for regulatory transcription factors and enzymes were clustered by expression patterns using hierarchical clustering (Fig. 10A). Upregulation of inhibitors *Tcf23* and *Icoslg* had the largest magnitude fold-change of the γδ T cell activation regulatory genes, likely driving the enrichment of this pathway (Fig. 10B & C). Multiple downregulated activators also contributed to downregulation and enrichment of this pathway: *Tcf3*, *Hes1*, *Syk*, *Gimap5*, *Sox13*, and notch. However, most of the activators, with the exception of *Sox13*, did not reach a threshold of FDR< 0.05 or fold-change > 2.

3.9. Differential expression of mitochondrial-related genes and mitochondrial copy number in female and male placental tissue

TCE-exposed female placental tissue was the only treatment group with downregulated pathways related to mitochondrial biogenesis and function including: 'cellular respiration' (enriched odds ratio=0.7, FDR=3 $\times 10^{-3}$), 'mitochondrial respiratory chain complex assembly' (enriched odds ratio=0.6, FDR=4 $\times 10^{-3}$), and 'mitochondrial transmembrane transport' (enriched odds ratio=0.5, FDR=3 $\times 10^{-3}$). Of the 38 differentially expressed genes that contributed to enrichment of these three pathways, the expression of 27 genes was completely reversed or attenuated in the TCE+NAC vs. control treatment group, compared to the TCE vs. control group (Fig. 11A).

Because mitochondrial genes were the only pathway NAC co-exposure attenuated TCE-induced differential expression, the number of mitochondria were further estimated for both female and male placental tissue. In female placental tissue (Fig. 11B), TCE exposure decreased the average number of mitochondria by 35% (P = 0.042), compared to control. Likewise, TCE+NAC decreased the average number of mitochondria by 38% (P = 0.027), compared to control, demonstrating that NAC attenuation of TCE effects on gene expression related to biogenesis did not extend to the number of mitochondria. In male placental tissue (Fig. 11 C), TCE exposure decreased the average number of mitochondria by 24% (P = 0.33), while TCE+NAC decreased mitochondria by 29% (P = 0.20).

3.10. Validation of gene expression of selected genes

Seven relevant genes were selected for gene expression validation with PCR (Fig. 12). Four genes were selected representing treatment-induced changes associated with endoplasmic reticulum stress: *Atf4*, *Trib3* and *Ddit3* (CHOP) from the PERK/ATF4-mediated branch of the UPR and *Atf6* from the ATF6 branch of the UPR. In the male TCE and TCE+NAC treatment groups, *Atf4* (Fig. 12 A) was significantly upregulated compared to controls (TCE: 2.0 FC, P = 3.9 $\times 10^{-02}$), (TCE+NAC: 2.6 FC, P < 0.001), but not in the female treatment groups. Likewise, *Trb3* (Fig. 12B) was upregulated in the male TCE (3.0 FC, P = not significant) and TCE+NAC (4.6 FC, P < 0.001) groups, although it was not significant in the TCE group, and no altered expression in the female treatment groups was measured. Although, *Ddit3* (CHOP) (Fig. 12 C)

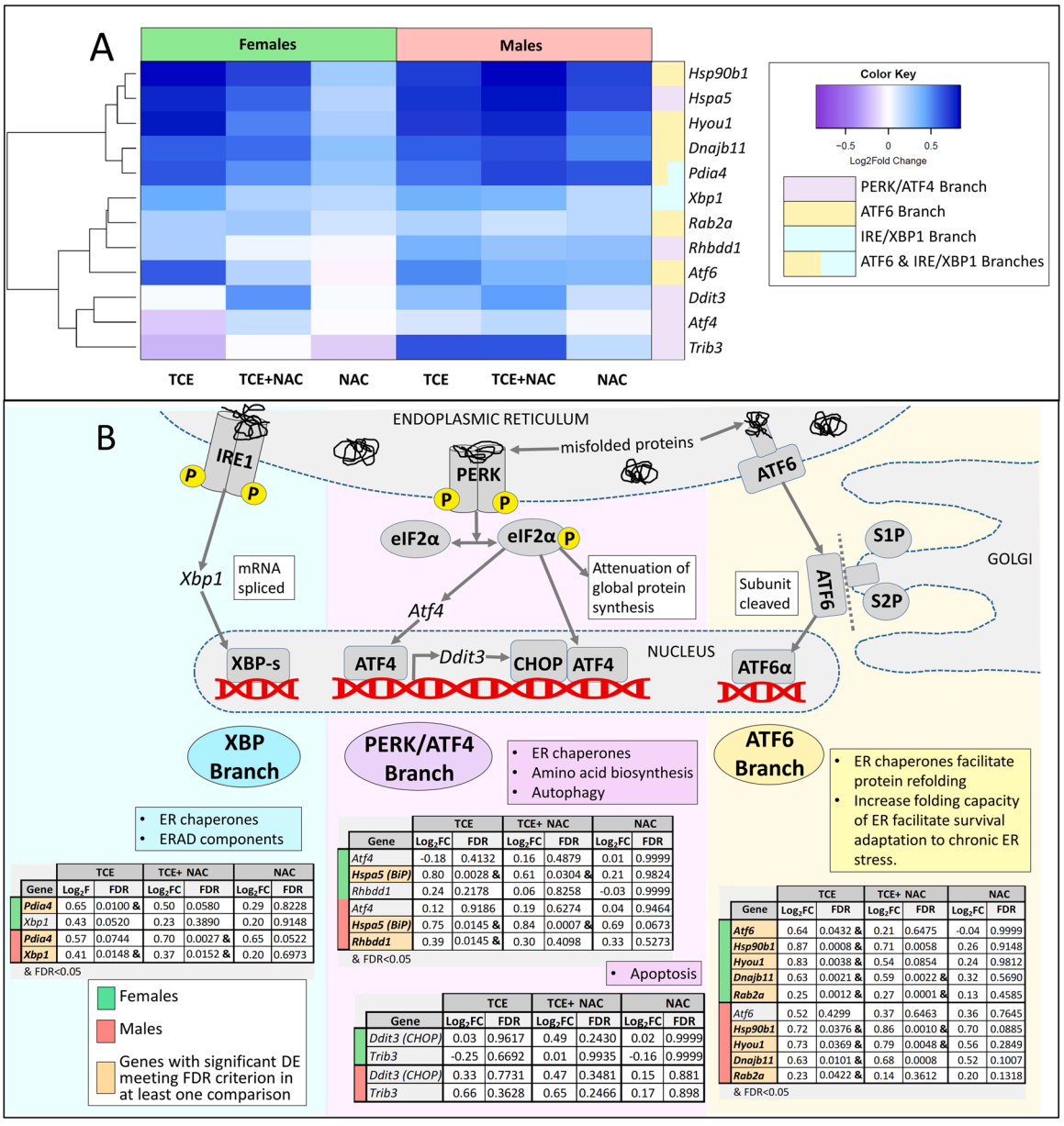

		TCE		TCE+ NAC		NAC	
	Gene	Log_2F	FDR	Log_2FC	FDR	Log_2FC	FDR
	Pdia4	0.65	0.0100 &	0.50	0.0580	0.29	0.8228
	Xbp1	0.43	0.0520	0.23	0.3890	0.20	0.9148
	Pdia4	0.57	0.0744	0.70	0.0027 &	0.65	0.0522
	Xbp1	0.41	0.0148 &	0.37	0.0152 &	0.20	0.6973

& FDR<0.05

		TCE		TCE+ NAC		NAC	
	Gene	Log_2FC	FDR	Log_2FC	FDR	Log_2FC	FDR
	Atf4	-0.18	0.4132	0.16	0.4879	0.01	0.9999
	Hspa5 (BiP)	0.80	0.0028 &	0.61	0.0304 &	0.21	0.9824
	Rhbdd1	0.24	0.2178	0.06	0.8258	-0.03	0.9999
	Atf4	0.12	0.9186	0.19	0.6274	0.04	0.9464
	Hspa5 (BiP)	0.75	0.0145 &	0.84	0.0007 &	0.69	0.0673
	Rhbdd1	0.39	0.0145 &	0.30	0.4098	0.33	0.5273

& FDR<0.05

		TCE		TCE+ NAC		NAC	
	Gene	Log_2FC	FDR	Log_2FC	FDR	Log_2FC	FDR
	Ddit3 (CHOP)	0.03	0.9617	0.49	0.2430	0.02	0.9999
	Trib3	-0.25	0.6692	0.01	0.9935	-0.16	0.9999
	Ddit3 (CHOP)	0.33	0.7731	0.47	0.3481	0.15	0.881
	Trib3	0.66	0.3628	0.65	0.2466	0.17	0.898

		TCE		TCE+ NAC		NAC	
	Gene	Log_2FC	FDR	Log_2FC	FDR	Log_2FC	FDR
	Atf6	0.64	0.0432 &	0.21	0.6475	-0.04	0.9999
	Hsp90b1	0.87	0.0008 &	0.71	0.0058	0.26	0.9148
	Hyou1	0.83	0.0038 &	0.54	0.0854	0.24	0.9812
	Dnajb11	0.63	0.0021 &	0.59	0.0022 &	0.32	0.5690
	Rab2a	0.25	0.0012 &	0.27	0.0001 &	0.13	0.4585
	Atf6	0.52	0.4299	0.37	0.6463	0.36	0.7645
	Hsp90b1	0.72	0.0376 &	0.86	0.0010 &	0.70	0.0885
	Hyou1	0.73	0.0369 &	0.79	0.0048 &	0.56	0.2849
	Dnajb11	0.63	0.0101 &	0.68	0.0008	0.52	0.1007
	Rab2a	0.23	0.0422 &	0.14	0.3612	0.20	0.1318

& FDR<0.05

Fig. 9. Exposure-induced endoplasmic reticulum stress across male and female placental tissues. One upregulated pathway, 'response to endoplasmic reticulum stress,' was enriched across all male and female treatment groups. A) Differential gene expression of 12 genes representing all three branches of the UPR were clustered by expression patterns using hierarchical clustering. Purple denotes PERK/ATF4 branch, yellow denotes ATF6 branch, turquoise denotes IRE/XBP1 branch, and half yellow-half turquoise represents both ATF6 and IRE XBP1 branches. B) Diagram illustrating the signaling and function of all three UPR branches with mini tables displaying differential gene expression log_2fold-change and FDR of relevant genes organized by UPR branch and stratified by sex. [&]Ampersand denotes significant difference compared to control ($P < 0.05$).

was also upregulated in the male TCE and TCE+NAC groups (TCE: 3.1 FC, P = not significant) (TCE+NAC: 2.7 FC, P = not significant), it was not statically significant and was not measured with PCR in the female treatment groups. These results lend additional evidence that collectively indicate male-specific activation of the PERK/ATF4-mediated branch of the UPR. Unlike gene associated with PERK/ATF4-mediated branch activation, *Atf6* (Fig. 12D) was upregulated in the male TCE and TCE+NAC groups (TCE: 3.9 FC, $P = 2.8 \times 10^{-3}$) (TCE+NAC: 2.2 FC, not significant) and in the female TCE+NAC group (TCE+NAC: 2.4 FC, not significant). *Atf6* was unchanged in the female TCE group. These results are largely consistent with RNA-seq results, together, indicating activation of the ATF6 branch of the UPR in both sexes.

Besides endoplasmic reticulum stress genes, two other genes were evaluated for changes in gene expression using PCR: *Il17* representing genes associated with $\gamma\delta$ T cell activation and *Sirt3* as a master regulator of mitochondrial stress response and biogenesis. *Il17* (Fig. 12E), the gene that produces the cytokine secreted by $\gamma\delta$ T cells, was upregulated in one treatment group, compared to controls, for each sex: the TCE group in males (TCE: 3.0 FC, $P = 5.9 \times 10^{-2}$) and the TCE+NAC group in females (TCE+NAC: 1.3 FC, not significant), although only the male TCE group was significant. Lastly, for *Sirt3* (Fig. 12 F), one of the genes that controls mitochondrial copy number, gene expression was upregulated in both the male TCE and TCE+NAC groups (TCE: 3.9 FC, $P = 1.9 \times 10^{-2}$) (TCE+NAC: 3.7 FC, $P = 2.4 \times 10^{-2}$), however, it was unchanged in the male treatment groups. Although some differences exist between RNA-seq and PCR results, perhaps due to library preparation or reference genes, overall, PCR validation supports the patterns of gene expression observed in the RNA-seq analyses.

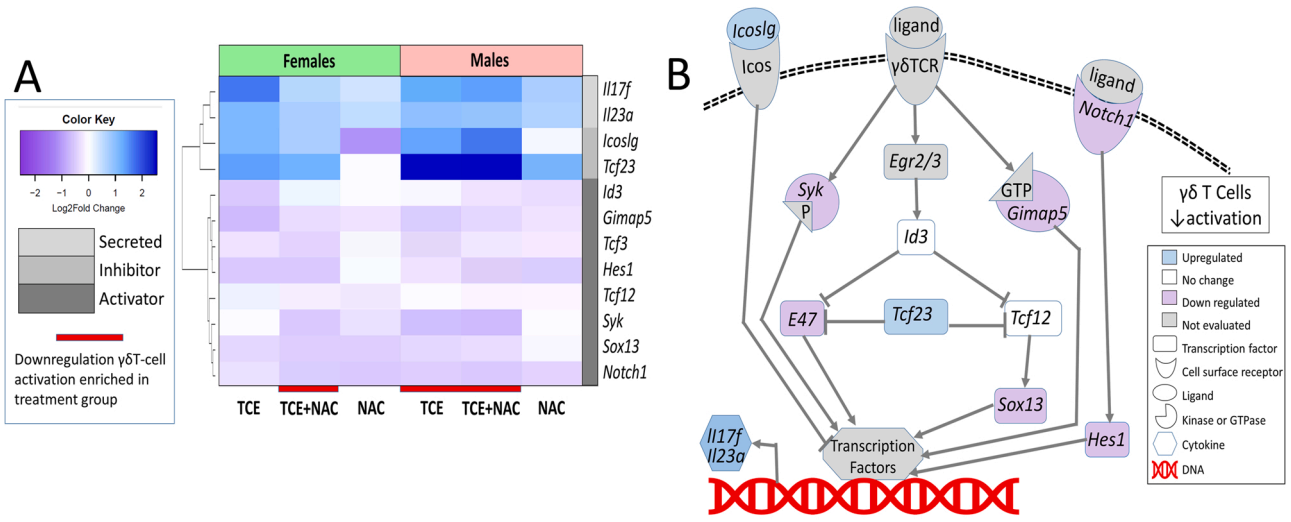

C

Sex:		Female						Male					
Treatment:		TCE		TCE+ NAC		NAC		TCE		TCE+ NAC		NAC	
Gene	Activator/ Inhibitor	Log_2Fold Change	FDR	Log_2Fold Change	FDR	Log_2Fold Change	FDR	Log_2Fold Change	FDR	Log_2Fold Change	FDR	Log_2Fold Change	FDR
Il17f	Secreted	1.64 #	0.1615	0.59	0.7168	0.40	0.9997	1.28 #	0.8123	1.37 #	0.7117	0.71	0.8686
Il23a	Secreted	1.07 #	0.1691	0.73	0.3803	0.50	0.9824	0.96	0.4195	0.91	0.3366	0.68	0.7586
Icoslg	inhibitor	1.10 #	0.5476	0.72	0.7495	-1.09	0.9812	1.35 #	0.6003	1.67 #	0.2438	0.11	0.9746
Tcf23	inhibitor	1.38 #	0.5059	1.19 #	0.6124	0.04	0.9997	2.55 #	0.0296 &	2.48 #	0.0154 &	1.14 #	0.7586
Tcf12	activator	0.18	0.4687	-0.16	0.5325	-0.20	0.8472	-0.03	0.9996	-0.12	0.9446	-0.11	0.9000
Id3	inhibitor	-0.51	0.5336	0.17	0.8857	0.01	0.8857	-0.10	0.9955	-0.25	0.9200	-0.33	0.8309
Tcf3	activator	-0.28	0.3048	-0.40	0.0968	-0.07	0.9997	-0.35	0.6037	-0.23	0.7954	-0.21	0.8167
Hes1	activator	-0.52	0.5908	-0.50	0.1537	0.05	0.9997	-0.25	0.7056	-0.46	0.0507	-0.49	0.1007
Syk	activator	-0.03	0.9650	-0.53	0.2559	-0.29	0.9845	-0.63	0.7797	-0.70	0.6110	-0.05	0.9795
Gimap5	activator	-0.68	0.3770	-0.32	0.7563	-0.25	0.8100	-0.49	0.3257	-0.36	0.4863	-0.25	0.8100
Sox13	activator	-0.36	0.1169	-0.47	0.0202 &	-0.47	0.1481	-0.37	0.0522	-0.34	0.0452 &	-0.10	0.8349
Notch1	activator	-0.29	0.6920	-0.49	0.4723	-0.52	0.8837	-0.45	0.7989	-0.50	0.6463	-0.40	0.8100

& FDR<0.05

Log_2FoldChange>1 or <-1

Females
Males
Genes with significant DE meeting FDR criterion in at least one comparison

Fig. 10. Exposure impacts on the gamma delta (γδ) T cell activation pathway across male and female placental tissue. The downregulated γδ T cell activation pathway was enriched in the female TCE+NAC group and the male TCE and TCE+NAC groups. A) Differential gene expression from 12 relevant genes representing activators, inhibitors and secretion products of γδ T cells are depicted in a heatmap and organized by hierarchical clustering. Light grey denotes secreted products, medium grey denotes inhibitors and dark grey denotes activators. B) Diagram illustrating relationships between activators and inhibitors involved in the regulation γδ T cells activation. White denotes no change in gene expression, blue denotes upregulation, purple denotes downregulation, and grey denotes genes expression not evaluated. C) Table displaying log_2fold-change and FDR for each gene organized by treatment group comparison and stratified by sex. [&]Ampersand denotes differential gene expression with FDR< 0.05. [#]Hashtag denotes differential gene expression with a log_2foldchange> 1 or < −1 [fold-change > 2].

4. Discussion

Exposure to the common environmental contaminant TCE during pregnancy is associated with reduced birth weight in several epidemiological studies (Forand et al., 2012; Ruckart et al., 2014). Our previous study reported that TCE exposure in pregnant rats decreased fetal weight and elevated oxidative stress biomarkers in placentae suggesting placental injury as a mechanism of TCE-induced adverse birth outcomes (Loch-Caruso et al., 2019). We built upon our previous findings by assessing TCE pre/co-exposure with the antioxidant NAC to investigate potential attenuation of TCE exposure effects. Recently, we observed TCE exposure caused male-specific reduced average fetal weight (Su et al., 2021). Moreover, TCE+NAC reduced fetal weight in both males and females, suggesting TCE+NAC may exacerbate rather than attenuate TCE-induced effects (Su et al., 2021). Here, we report TCE- and/or NAC-induced changes to gene expression in male and female rat placental tissues, identifying pathways of dysregulation that may contribute to mechanisms of TCE-induced adverse birth outcomes.

4.1. Endoplasmic reticulum stress in rat placental tissue

One of the most notable findings from the present differential gene expression analyses was the enrichment of the upregulated 'response to endoplasmic reticulum stress' pathway because it was enriched across all treatment groups for both sexes. Moreover, to our knowledge, this is the first study to report TCE-induced endoplasmic reticulum stress in an in vivo study. When misfolded proteins accumulate in the lumen of the endoplasmic reticulum resulting in endoplasmic reticulum stress, all three UPR branches are simultaneously triggered, each with a distinctive role (Okada et al., 2002). Despite across-the-board enrichment of the endoplasmic reticulum stress pathway, there were important nuanced differences in the relevant gene expression profiles of some experimental groups based on treatment. For example, the male and female NAC groups had no significant differential gene expression, whereas the male and female TCE and TCE+NAC groups had many differentially expressed genes that met FDR criterion. Moreover, changes in TCE- and TCE+NAC-induced gene expression were primarily driven by *Atf6* upregulation, as demonstrated by significant overrepresentation of ATF6 gene targets among differentially expressed genes in these groups. This expression pattern is important because the ATF6 UPR branch promotes long-term adaptation by regulating the gene expression of ER chaperones that facilitate an enhanced capacity to fold/refold naïve proteins during synthesis (Adachi et al., 2008; Okada et al., 2002). Additionally, prevalent ATF6 activation indicates adaptation to prolonged stress because ATF6 mRNA transcripts are more stable and last longer than other UPR branches (Rutkowski et al., 2006). These treatment-specific results suggest that the response to endoplasmic reticulum stress in TCE- and TCE+NAC-exposed placental tissue was largely driven by cellular adaptation via the ATF 6 branch of the UPR.

In addition to differences in the gene expression patterns of

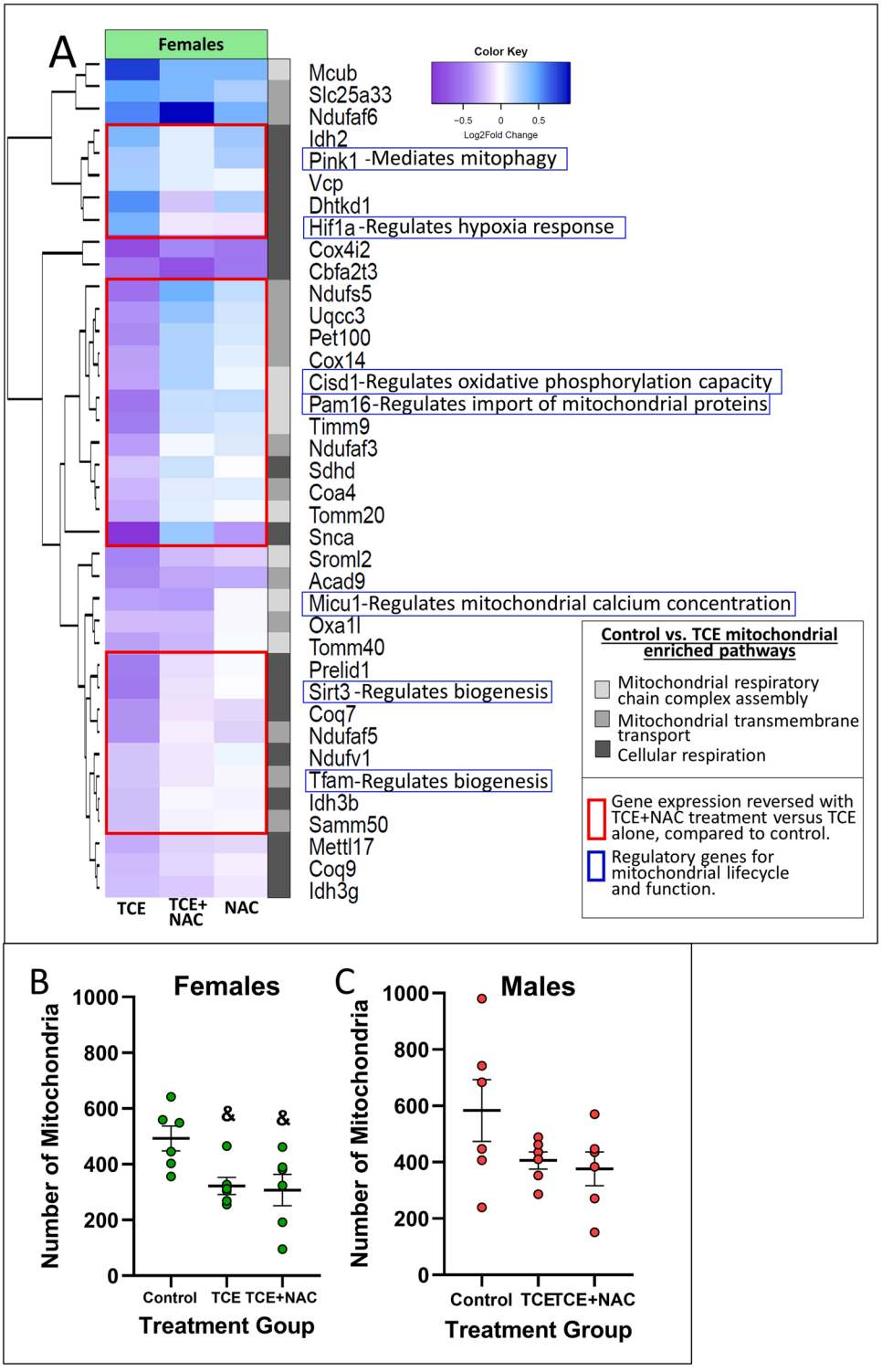

Fig. 11. Exposure-induced differential expression of mitochondrial-related genes and mitochondrial copy number. Three downregulated mitochondrial-associated pathways, 'cellular respiration (dark grey),' 'mitochondrial respiratory chain complex assembly (light grey),' and 'mitochondrial transmembrane transport (medium grey),' were enriched only in the female TCE treatment group compared to control. A) Differential gene expression from the 38 genes driving enrichment of the three pathways in the TCE group are depicted in a heatmap and organized by hierarchical clustering. Genes outlined by red boxes within heatmap denote TCE-induced gene expression changes reversed or attenuated by TCE pre-/co-treatment with NAC. Blue boxes around gene names denote genes involved in regulating mitochondrial function and lifecycle processes. To determine if gene expression changes carried functional consequences, the number of mitochondria in B) female and C) male (for comparison) placental tissues were estimated by measuring genomic DNA of a mitochondrial-encoded gene and a nuclear-encoded gene and calculated the ratio. Horizontal lines represent mean±SD. Data were analyzed by one-way ANOVA with posthoc Tukey's multiple comparisons. [&]Ampersand denotes significant difference compared to control ($P < 0.05$).

endoplasmic reticulum stress-associated genes between treatment groups, there were also specific differences in expression patterns between sexes. For male placentae, but not females, the TCE group had significant overrepresentation of ATF4 gene targets. ATF4, part of the UPR PERK/ATF4 branch, controls a complex signaling network that promotes a largely pro-adaptive intracellular response to stress through selective gene expression and global protein synthesis attenuation (Pakos-Zebrucka et al., 2016; Wortel et al., 2017). If prolonged or severe stress persists, then protein synthesis may resume and ATF4 dimerizes with CHOP to upregulate pro-apoptotic genes (Han et al., 2013). Here, both the male TCE and TCE+NAC groups had several important ATF4/CHOP gene targets upregulated including *Trib3,* a gene that codes for a key protein involved endoplasmic reticulum stress-induced (Ohoka et al., 2005; Ord and Ord, 2005), which was upregulated in both RNA-seq analysis and PCR validation, although only meeting statically significant criterion in PCR validation. Activation of the PERK/ATF4 branch of the UPR is consistent with our previous results demonstrating the same physiological stress response in a human placental cell line and first-trimester placental villous explants exposed to the TCE metabolite DCVC in vitro (Elkin et al., 2021). Male-specific involvement of the UPR

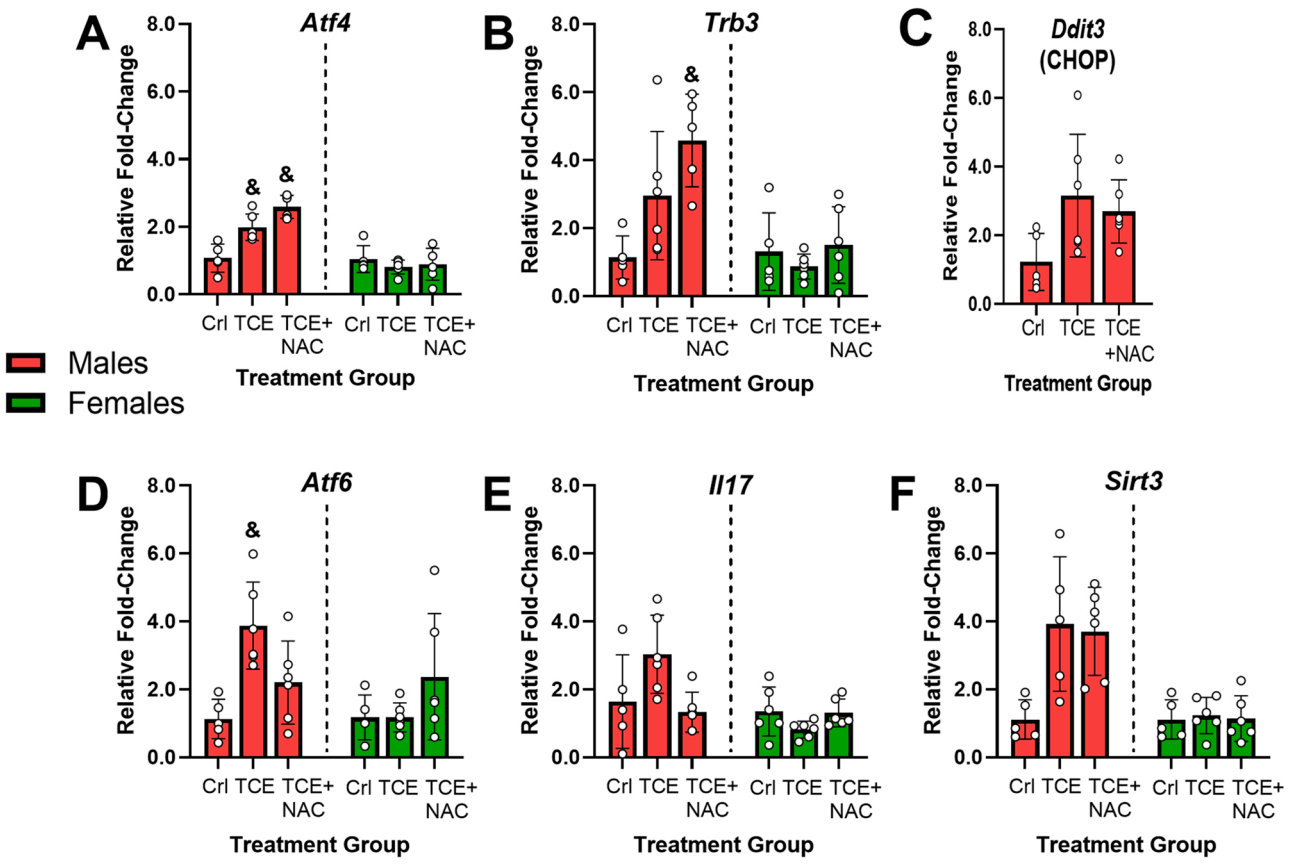

Fig. 12. Validation of gene expression of selected genes. Seven relevant genes were selected for gene expression validation with PCR. Three genes representing the PERK/ATF4 branch of the UPR: A) *Atf4*, B) *Trb3*, C) *Ddit3* (CHOP); One gene representing the ATF6 branch of the UPR: D) *Atf6*; One gene representing the $\gamma\delta$ T cell activation pathway: E) *Il17f*; and one gene representing mitochondrial biogenesis: F) *Sirt3*. Horizontal lines represent mean±SD. Data were analyzed by one-way ANOVA with posthoc Tukey's multiple comparisons. Green color denotes PCR results for female placental tissue and red color represents male placental tissue. [&]Ampersand denotes significant relative fold-change difference compared to control ($P < 0.05$).

PERK/ATF4 branch in response to ER stress may be an underlying mechanism contributing to the observed decrease in male fetal weights observed in TCE and TCE+NAC-treated rats (Su et al., 2021). Indeed, endoplasmic reticulum stress involving the PERK/ATF4 branch of the UPR is associated with early-onset preeclampsia (Burton et al., 2009; Fu et al., 2015) and intrauterine growth restriction in humans (Fu et al., 2015).

4.2. Mitochondrial stress in rat placental tissue

In addition to endoplasmic reticulum stress, pathway analysis further revealed female-specific enrichment of multiple downregulated pathways associated with mitochondrial biogenesis and function in placental tissue. There was also a decrease in the number of mitochondria measured in the TCE and TCE+NAC groups, compared to controls, in both male and female tissue, although data for males was not significant. As the primary organelle responsible for cellular energy generation in the form of ATP, dynamic and flexible mitochondrial function plays an essential role in the rapid growth and development of the placenta throughout pregnancy (Sferruzzi-Perri et al., 2019). Mitochondrial disruptions are thought to play a role in the pathophysiology of pregnancy disorders. Reactive oxygen species and lipid peroxidation generated by mitochondrial perturbations and alterations in the number of mitochondria in placental cells have been observed in pregnancy disorders involving abnormal placental development, as previously reviewed (Gupta et al., 2005; Holland et al., 2017). Our findings in female placenta indicating downregulation of regulatory genes associated with cellular respiration activity and mitochondrial biogenesis are consistent with our previous report of decreased cellular respiration and number of mitochondria in placental cells exposed to the TCE metabolite DCVC in vitro (Elkin et al., 2019), and in previous reports of DCVC-induced mitochondrial dysfunction in proximal tubal kidney cells (Lash et al., 2003; Lash et al., 1995; van de Water et al., 1994; van de Water et al., 1993; Xu et al., 2008). The exposure-induced changes to mitochondrial-associated genes reported here, along with previous evidence, together, strongly suggest the involvement of mitochondria in the placental response to maternal TCE and NAC exposure. Another report we recently published detailed arginine metabolism deficiency in the amniotic fluid of rats from our study (Su et al., 2022). However, it remains unclear what role, if any, mitochondrial perturbation may play in the reduced male fetal weights observed in our first published report from our follow-up TCE and/or NAC rat exposure study (Su et al., 2021). One hypothesis that may explain female -specific downregulation in genes involved in mitochondrial function, as well as male-specific reduced fetal weights is an adaptive response of the female placenta to spare limited nutrition for the fetus, with a failure of the male placenta to adapt in similar fashion resulting in reduced fetal weight. Regardless, the findings of this study warrant further scrutiny as to how mitochondrial dysfunction may be involved in the TCE toxic mechanism of action.

4.3. Immune system perturbations in rat placental tissue

Differential gene expression caused by TCE and TCE+NAC exposure in male and female rat placentae resulted in the enrichment of multiple different pathways associated with the immune system and response. The proper regulation of placental immune activity is essential for

normal pregnancy progression and fetal development because it promotes maternal immune tolerance of the semi-allogenic fetus and simultaneously promotes immune activation against pathogenic infection (Than et al., 2019). Although the placenta is of fetal origin, it is well-documented that maternal immune cells are capable of crossing the maternal-fetal syncytiotrophoblast barrier infiltrating placental villi, especially during abnormal placental inflammation (Kim et al., 2015; Myerson et al., 2006; Redline and Patterson, 1993). For this reason, we acknowledge that enriched immune system pathways could be caused by differential gene expression in maternal cells, fetal cells, or both in placental tissue.

One particular set of downregulated pathways reported here indicate the activation of two specific types of lymphocytes, γδ T cells and B cells, which evidence shows play a pivotal role in localized immunomodulation and/or host defense at the maternal-fetal interface during pregnancy (Fettke et al., 2016; Mincheva-Nilsson, 2003; Pinget et al., 2016). The 'activation of γδ T cells' and/or 'regulation of γδ T cells activation' pathways were downregulated in the male TCE and TCE+NAC groups and female TCE+NAC group, while the 'B cell activation' and/or 'B cell receptor signaling' pathways were downregulated in the male and female TCE+NAC groups. Although Gene Ontology does not specify γδ T cell subgroups in pathway enrichment, two γδ T cell subtypes have been identified in high abundance in the maternal decidua (Guzman-Genuino and Diener, 2017; Nagaeva et al., 2002) and placental villi (Bonney et al., 2000; Pinget et al., 2016), γδ T17 cells and regulatory γδ T cell (γδ Treg) (Solano, 2019).

γδ T17 cells primarily secrete IL-17a and IL-17 f (Chang and Dong, 2009), isoforms of the pro-inflammatory cytokine IL-17 implicated in pathogen defense (Curtis and Way, 2009). Here, despite downregulation of the γδ T cell activation pathway in multiple exposure groups, the *Il-17 f* gene (not meeting FDR criterion) was upregulated in the same groups, suggesting downregulated γδ T activation may be a secondary response via a negative feedback loop responding to upregulated *Il-17 f* and *Il-23a* - itself, also upregulated (not meeting FDR criterion) (Purvis et al., 2014; Silverpil et al., 2013). During pregnancy, elevated IL-17 and IL-23 are associated with preeclampsia and placental insufficiency (Cornelius and Lamarca, 2014; Darmochwal-Kolarz et al., 2017; Dhillion et al., 2012), which may be a mechanism by which TCE and/or co-exposure to NAC contribute to adverse birth outcomes.

Because the placenta and fetus are genetically distinct from the mother, localized immunomodulation at the maternal-fetal interface in the placenta facilitates critical immune tolerance between maternal and fetal tissues. The other type of T cell detected in placenta, γδ Tregs, as well as B cells, have been shown to selectively suppress immune system activity in a compartment-specific manner through downregulation of natural killer cells and upregulation of placental trophoblasts with the anti-inflammatory cytokines IL-10, IL-4 and TGF-β (Fettke et al., 2016; Guzman-Genuino and Diener, 2017; Mincheva-Nilsson, 2003; Nagaeva et al., 2002; Suzuki et al., 1995). IL-10 deficiency has been linked to pregnancy complications such as preeclampsia (Chatterjee et al., 2014; Hennessy et al., 1999) and chronic inflammation (Murphy et al., 2005). Although we did not detect differential gene expression in these specific cytokines, TCE and TCE+NAC-induced downregulation of γδ Tregs activation may impair immunomodulation at the maternal-fetal interface and promote an unchecked inflammatory response via other undetermined anti-inflammatory cytokines.

Consistent with potentially impaired immunomodulation, the 'chronic inflammation' pathway was upregulated and enriched in the male and female TCE+NAC groups. Chronic inflammation, distinct from acute inflammation, is a prolonged low-grade inflammatory response characterized by infiltration of lymphocytes and macrophages combined with variety of proinflammatory signaling chemicals such as cytokines, chemokines and c-reactive protein (Furman et al.,2019). Chronic inflammation in the placenta typically involves both maternal and fetal immune system cells, depending on the location in the placenta (Katzman, 2015; Kim et al., 2015; Myerson et al., 2006). In both male and female rat placenta, enrichment of 'chronic inflammatory response' pathway was driven by upregulation of *Il1b (*did not meet FDR criterion), which codes for the proinflammatory cytokine IL-1b, and *S100a9s (*did not meet FDR criterion), which codes for the proinflammatory regulatory protein MRP14. Consistent with our previous results demonstrating reduced fetal weight in male and female TCE+NAC-exposed fetuses (Su et al., 2021) elevated IL-1b has been shown to significantly decrease birth weight in humans and mice (Reis et al., 2020). Moreover, IL-1b also increased the rate of preterm birth and fetal mortality in mice (Romero et al., 1991).

5. Conclusion

In summary, we used transcriptomics and pathway enrichment analyses in a rat model of pregnancy to identify and reaffirm specific genes, biological processes and molecular signaling pathways altered in placenta in response to TCE and/or NAC exposure during pregnancy. Furthermore, PCR validated differential gene expression results and mitochondrial content was measured as a proxy for the number of mitochondria altered in placental tissue. Overall, female placental tissues demonstrated a more robust transcriptional response to TCE and/or NAC exposure than male tissues. Furthermore, NAC did not attenuate TCE-induced effects on gene expression except for some mitochondrial-associated genes which did not attenuate TCE effects on the number of mitochondria. Multiple pathways were enriched in both sexes including downregulated 'γδ T cell activation' and upregulated 'response to endoplasmic reticulum stress.' The endoplasmic reticulum pathway was enriched in all male and female treatment groups, compared to controls, however, in female, the ATF6 branch of the UPR drove enrichment, whereas in males, both the ATF6 and PERK/ATF4 branch drove enrichment. Sex-specific nuanced responses to endoplasmic reticulum stress and mitochondrial dysfunction, as well as a presumptive larger internal dose of glutathione conjugation metabolites, may explain, in part, why male fetuses had reduced fetal weights compared to female fetuses, as reported in our previous paper (Su et al., 2021). Our findings also contribute to the biological plausibility of TCE-induced placental toxicity, providing a compelling rationale for further studies into the effect of TCE and its metabolites on placental cells. Future studies will pay particularly attention to specific placental cell types that may contribute to the bulk tissue transcriptomic results reported here.

Accession number

RNA-seq fastq and featureCount files are publicly available for download at SRA.

Gene Expression Omnibus (GEO) accession number: GSE168232.

CODE on Github https://github.com/bakulskilab/rat_tce_rnaseq.

Funding

This work was supported by the National Institute of Environmental Health Sciences, National Institutes of Health (Grant Nos. P42 ES017198, P30 ES017885, R01 ES025574, R01 ES025531, T32 ES007062 and R01 ES028802); National Institute of Diabetes and Digestive Kidney Diseases (Grant Nos. R01 DK107535 and T32 DK071212); National Institute of Aging (Grant Nos. R01 AG055406 and P30 AG053760). The content is solely the responsibility of the authors and does not necessarily represent the official views of the NIEHS, NIDDK, NIA, or NIH.

Declaration of Competing Interest

The authors declare that they have no known competing financial interests or personal relationships that could have appeared to influence the work reported in this paper.

Data Availability

RNA-seq fastq and featureCount files are publicly available for download at SRA. Gene Expression Omnibus (GEO) accession number: GSE168232. CODE on Github https://github.com/bakulskilab/rat_tce_rnaseq.

Acknowledgments

We thank Andrea Ruszala of the University of Michigan Advanced Genomics Core for her assistance with library preparation and RNA-seq. We gratefully acknowledge Faith Bjork and Kyle Campbell, JeAnna Redd and Molly Mulcahy for assistance with learning new laboratory techniques and for helpful scientific discussions, and Monica Smolinski for general lab assistance.

Appendix A. Supporting information

Supplementary data associated with this article can be found in the online version at doi:10.1016/j.tox.2022.153371.

References

Adachi, Y., Yamamoto, K., Okada, T., Yoshida, H., Harada, A., Mori, K., 2008. ATF6 is a transcription factor specializing in the regulation of quality control proteins in the endoplasmic reticulum. Cell Struct. Funct. 33, 75–89.

Agency for Toxic Substances and Disease Registry. 2007. Trichloroethylene Toxicity: What are the U.S. Standards for Trichloroethylene Exposure? In: E.H.a.M.E. Agency for Toxic Substances and Disease Registry (ATSDR) (Ed), Atlanta, GA.

Ain, R., Konno, T., Canham, L.N., Soares, M.J., 2006. Phenotypic analysis of the rat placenta. Methods Mol. Med 121, 295–313.

Anders, S., Huber, W., 2010. Differential expression analysis for sequence count data. Genome Biol. 11, R106.

Andrews, S., 2010. FastQC: a quality control tool for high throughput sequence data. Bahraham Bioinformaticz.

Benjamini, Y., Hochberg, Y., 1995. Controlling the false discovery rate: a practical and powerful approach to multiple testing. J. R. Stat. Soc. Ser. B 57, 289–300.

Bonney, E.A., Pudney, J., Anderson, D.J., Hill, J.A., 2000. Gamma-delta T cells in midgestation human placental villi. Gynecol. Obstet. Invest. 50, 153–157.

Bromati, C.R., Lellis-Santos, C., Yamanaka, T.S., Nogueira, T.C., Leonelli, M., Caperuto, L.C., Gorjao, R., Leite, A.R., Anhe, G.F., Bordin, S., 2011. UPR induces transient burst of apoptosis in islets of early lactating rats through reduced AKT phosphorylation via ATF4/CHOP stimulation of TRB3 expression. Am. J. Physiol. Regul. Integr. Comp. Physiol. 300, R92–R100.

Burton, G.J., Fowden, A.L., 2015. The placenta: a multifaceted, transient organ. Philos. Trans. R. Soc. Lond. B Biol. Sci. 370, 20140066.

Burton, G.J., Yung, H.W., Cindrova-Davies, T., Charnock-Jones, D.S., 2009. Placental endoplasmic reticulum stress and oxidative stress in the pathophysiology of unexplained intrauterine growth restriction and early onset preeclampsia. Placenta 30 (Suppl A), S43–S48.

Chang, E.Y., Barbosa, E., Paintlia, M.K., Singh, A., Singh, I., 2005. The use of N-acetylcysteine for the prevention of hypertension in the reduced uterine perfusion pressure model for preeclampsia in Sprague-Dawley rats. Am. J. Obstet. Gynecol. 193, 952–956.

Chang, S.H., Dong, C., 2009. IL-17F: regulation, signaling and function in inflammation. Cytokine 46, 7–11.

Chatterjee, P., Chiasson, V.L., Bounds, K.R., Mitchell, B.M., 2014. Regulation of the anti-inflammatory cytokines interleukin-4 and interleukin-10 during pregnancy. Front. Immunol. 5, 253.

Chen, Y., Gui, D., Chen, J., He, D., Luo, Y., Wang, N., 2014. Down-regulation of PERK-ATF4-CHOP pathway by Astragaloside IV is associated with the inhibition of endoplasmic reticulum stress-induced podocyte apoptosis in diabetic rats. Cell Physiol. Biochem 33, 1975–1987.

Chiu, W.A., Jinot, J., Scott, C.S., Makris, S.L., Cooper, G.S., Dzubow, R.C., Bale, A.S., Evans, M.V., Guyton, K.Z., Keshava, N., Lipscomb, J.C., Barone Jr., S., Fox, J.F., Gwinn, M.R., Schaum, J., Caldwell, J.C., 2013. Human health effects of trichloroethylene: key findings and scientific issues. Environ. Health Perspect. 121, 303–311.

Cornelius, D.C., Lamarca, B., 2014. TH17- and IL-17- mediated autoantibodies and placental oxidative stress play a role in the pathophysiology of pre-eclampsia. Minerva Ginecol. 66, 243–249.

Curtis, M.M., Way, S.S., 2009. Interleukin-17 in host defence against bacterial, mycobacterial and fungal pathogens. Immunology 126, 177–185.

Darmochwal-Kolarz, D., Michalak, M., Kolarz, B., Przegalinska-Kalamucka, M., Bojarska-Junak, A., Sliwa, D., Oleszczuk, J., 2017. The role of interleukin-17, interleukin-23, and transforming growth factor-beta in pregnancy complicated by placental insufficiency. Biomed. Res. Int. 2017, 6904325.

Dhillion, P., Wallace, K., Herse, F., Scott, J., Wallukat, G., Heath, J., Mosely, J., Martin Jr., J.N., Dechend, R., LaMarca, B., 2012. IL-17-mediated oxidative stress is an important stimulator of AT1-AA and hypertension during pregnancy. Am. J. Physiol. Regul. Integr. Comp. Physiol. 303, R353–R358.

Dobin, A., Davis, C.A., Schlesinger, F., Drenkow, J., Zaleski, C., Jha, S., Batut, P., Chaisson, M., Gingeras, T.R., 2013. STAR: ultrafast universal RNA-seq aligner. Bioinformatics 29, 15–21.

Elkin, E.R., Bridges, D., Loch-Caruso, R., 2019. The trichloroethylene metabolite S-(1,2-dichlorovinyl)-L-cysteine induces progressive mitochondrial dysfunction in HTR-8/SVneo trophoblasts. Toxicology, 152283.

Elkin, E.R., Harris, S.M., Su, A.L., Lash, L.H., Loch-Caruso, R., 2020. Placenta as a target of trichloroethylene toxicity. Environ. Sci. Process Impacts.

Elkin, E.R., Bakulski, K.M., Colacino, J.A., Bridges, D., Kilburn, B.A., Armant, D.R., Loch-Caruso, R., 2021. Transcriptional profiling of the response to the trichloroethylene metabolite S-(1,2-dichlorovinyl)-L-cysteine revealed activation of the eIF2alpha/ATF4 integrated stress response in two in vitro placental models. Arch. Toxicol. 95, 1595–1619.

Ewels, P., Magnusson, M., Lundin, S., Kaller, M., 2016. MultiQC: summarize analysis results for multiple tools and samples in a single report. Bioinformatics 32, 3047–3048.

Fettke, F., Schumacher, A., Canellada, A., Toledo, N., Bekeredjian-Ding, I., Bondt, A., Wuhrer, M., Costa, S.D., Zenclussen, A.C., 2016. Maternal and fetal mechanisms of b cell regulation during pregnancy: human chorionic gonadotropin stimulates B cells to produce IL-10 while alpha-fetoprotein drives them into apoptosis. Front Immunol. 7, 495.

Fisher, J.W., Whittaker, T.A., Taylor, D.H., Clewell 3rd, H.J., Andersen, M.E., 1989. Physiologically based pharmacokinetic modeling of the pregnant rat: a multiroute exposure model for trichloroethylene and its metabolite, trichloroacetic acid. Toxicol. Appl. Pharm. 99, 395–414.

Fisher, J.W., Channel, S.R., Eggers, J.S., Johnson, P.D., MacMahon, K.L., Goodyear, C.D., Sudberry, G.L., Warren, D.A., Latendresse, J.R., Graeter, L.J., 2001. Trichloroethylene, trichloroacetic acid, and dichloroacetic acid: do they affect fetal rat heart development? Int J. Toxicol. 20, 257–267.

Forand, S.P., Lewis-Michl, E.L., Gomez, M.I., 2012. Adverse birth outcomes and maternal exposure to trichloroethylene and tetrachloroethylene through soil vapor intrusion in New York State. Environ. Health Perspect. 120, 616–621.

Fu, J., Zhao, L., Wang, L., Zhu, X., 2015. Expression of markers of endoplasmic reticulum stress-induced apoptosis in the placenta of women with early and late onset severe pre-eclampsia. Taiwan J. Obstet. Gynecol. 54, 19–23.

Fukami, G., Hashimoto, K., Koike, K., Okamura, N., Shimizu, E., Iyo, M., 2004. Effect of antioxidant N-acetyl-L-cysteine on behavioral changes and neurotoxicity in rats after administration of methamphetamine. Brain Res. 1016, 90–95.

Furman, D., Campisi, J., Verdin, E., Carrera-Bastos, P., Targ, S., Franceschi, C., Ferrucci, L., Gilroy, D.W., Fasano, A., Miller, G.W., Miller, A.H., Mantovani, A., Weyand, C.M., Barzilai, N., Goronzy, J.J., Rando, T.A., Effros, R.B., Lucia, A., Kleinstreuer, N., Slavich, G.M., 2019. Chronic inflammation in the etiology of disease across the life span. Nat. Med. 25, 1822–1832.

Furukawa, S., Hayashi, S., Usuda, K., Abe, M., Hagio, S., Ogawa, I., 2011. Toxicological pathology in the rat placenta. J. Toxicol. Pathol. 24, 95–111.

Ghantous, H., Danielsson, B.R., Dencker, L., Gorczak, J., Vesterberg, O., 1986. Trichloroacetic acid accumulates in murine amniotic fluid after tri- and tetrachloroethylene inhalation. Acta Pharm. Toxicol. 58, 105–114.

Grigsby, P.L., 2016. Animal models to study placental development and function throughout normal and dysfunctional human pregnancy. Semin Reprod. Med 34, 11–16.

Gupta, S., Agarwal, A., Sharma, R.K., 2005. The role of placental oxidative stress and lipid peroxidation in preeclampsia. Obstet. Gynecol. Surv. 60, 807–816.

Guzman-Genuino, R.M., Diener, K.R., 2017. Regulatory B cells in pregnancy: lessons from autoimmunity, graft tolerance, and cancer. Front Immunol. 8, 172.

Han, J., Back, S.H., Hur, J., Lin, Y.H., Gildersleeve, R., Shan, J., Yuan, C.L., Krokowski, D., Wang, S., Hatzoglou, M., Kilberg, M.S., Sartor, M.A., Kaufman, R.J., 2013. ER-stress-induced transcriptional regulation increases protein synthesis leading to cell death. Nat. Cell Biol. 15, 481–490.

Hartley, S.W., Mullikin, J.C., 2015. QoRTs: a comprehensive toolset for quality control and data processing of RNA-Seq experiments. BMC Bioinforma. 16, 224.

Healy, T.E., Poole, T.R., Hopper, A., 1982. Rat fetal development and maternal exposure to trichloroethylene 100 p.p.m. Br. J. Anaesth. 54, 337–341.

Hennessy, A., Pilmore, H.L., Simmons, L.A., Painter, D.M., 1999. A deficiency of placental IL-10 in preeclampsia. J. Immunol. 163, 3491–3495.

Heydari, M., Ahmadizadeh, M. and Ahmadi Angali, K., 2017. Ameliorative effect of vitamin E on trichloroethylene-induced nephrotoxicity in rats. J. Nephropathol. 6, 168–173.

Holland, O., Dekker Nitert, M., Gallo, L.A., Vejzovic, M., Fisher, J.J., Perkins, A.V., 2017. Review: placental mitochondrial function and structure in gestational disorders. Placenta 54, 2–9.

Horowitz, R.S., Dart, R.C., Jarvie, D.R., Bearer, C.F., Gupta, U., 1997. Placental transfer of N-acetylcysteine following human maternal acetaminophen toxicity. J. Toxicol.: Clin. Toxicol. 35, 447–451.

Kalisch-Smith, J.I., Simmons, D.G., Dickinson, H., Moritz, K.M., 2017. Review: sexual dimorphism in the formation, function and adaptation of the placenta. Placenta 54, 10–16.

Katzman, P.J., 2015. Chronic inflammatory lesions of the placenta. Semin Perinatol. 39, 20–26.

Kim, C.J., Romero, R., Chaemsaithong, P., Kim, J.S., 2015. Chronic inflammation of the placenta: definition, classification, pathogenesis, and clinical significance. Am. J. Obstet. Gynecol. 213, S53–S69.

Laham, S., 1970. Studies on placental transfer. Trichlorethylene. IMS Ind. Med Surg. 39, 46–49.

Lash, L.H., Xu, Y., Elfarra, A.A., Duescher, R.J., Parker, J.C., 1995. Glutathione-dependent metabolism of trichloroethylene in isolated liver and kidney cells of rats and its role in mitochondrial and cellular toxicity. Drug Metab. Dispos. 23, 846–853.
Lash, L.H., Fisher, J.W., Lipscomb, J.C., Parker, J.C., 2000. Metabolism of trichloroethylene. Environ. Health Perspect. 108 (Suppl 2), 177–200.
Lash, L.H., Putt, D.A., Hueni, S.E., Krause, R.J., Elfarra, A.A., 2003. Roles of necrosis, Apoptosis, and mitochondrial dysfunction in S-(1,2-dichlorovinyl)-L-cysteine sulfoxide-induced cytotoxicity in primary cultures of human renal proximal tubular cells. J. Pharm. Exp. Ther. 305, 1163–1172.
Lasram, M.M., Dhouib, I.B., Annabi, A., El Fazaa, S., Gharbi, N., 2015. A review on the possible molecular mechanism of action of N-acetylcysteine against insulin resistance and type-2 diabetes development. Clin. Biochem 48, 1200–1208.
Lee, C., Patil, S., Sartor, M.A., 2016. RNA-Enrich: a cut-off free functional enrichment testing method for RNA-seq with improved detection power. Bioinformatics 32, 1100–1102.
Liao, Y., Smyth, G.K., Shi, W., 2014. featureCounts: an efficient general purpose program for assigning sequence reads to genomic features. Bioinformatics 30, 923–930.
Liu, M., Choi, D.Y., Hunter, R.L., Pandya, J.D., Cass, W.A., Sullivan, P.G., Kim, H.C., Gash, D.M., Bing, G., 2010. Trichloroethylene induces dopaminergic neurodegeneration in Fisher 344 rats. J. Neurochem 112, 773–783.
Livak, K.J., Schmittgen, T.D., 2001. Analysis of relative gene expression data using real-time quantitative PCR and the 2(-Delta Delta C(T)) method. Methods 25, 402–408.
Loch-Caruso, R., Hassan, I., Harris, S.M., Kumar, A., Bjork, F., Lash, L.H., 2019. Trichloroethylene exposure in mid-pregnancy decreased fetal weight and increased placental markers of oxidative stress in rats. Reprod. Toxicol. 83, 38–45.
Loof, T., Kramer, S., Gaedeke, J., Neumayer, H.H., Peters, H., 2016. IL-17 expression in the time course of acute anti-Thy1 glomerulonephritis. PLoS One 11, e0156480.
Love, M.I., Huber, W., Anders, S., 2014. Moderated estimation of fold change and dispersion for RNA-seq data with DESeq2. Genome Biol. 15, 550.
Luo, H., Zhou, M., Ji, K., Zhuang, J., Dang, W., Fu, S., Sun, T., Zhang, X., 2017. Expression of Sirtuins in the Retinal Neurons of Mice, Rats, and Humans. Front Aging Neurosci. 9, 366.
Matys, V., Fricke, E., Geffers, R., Gossling, E., Haubrock, M., Hehl, R., Hornischer, K., Karas, D., Kel, A.E., Kel-Margoulis, O.V., Kloos, D.U., Land, S., Lewicki-Potapov, B., Michael, H., Munch, R., Reuter, I., Rotert, S., Saxel, H., Scheer, M., Thiele, S., Wingender, E., 2003. TRANSFAC: transcriptional regulation, from patterns to profiles. Nucleic Acids Res 31, 374–378.
Matys, V., Kel-Margoulis, O.V., Fricke, E., Liebich, I., Land, S., Barre-Dirrie, A., Reuter, I., Chekmenev, D., Krull, M., Hornischer, K., Voss, N., Stegmaier, P., Lewicki-Potapov, B., Saxel, H., Kel, A.E., Wingender, E., 2006. TRANSFAC and its module TRANSCompel: transcriptional gene regulation in eukaryotes. Nucleic Acids Res 34, D108–D110.
Mincheva-Nilsson, L., 2003. Pregnancy and gamma/delta T cells: taking on the hard questions. Reprod. Biol. Endocrinol. 1, 120.
Murphy, S.P., Fast, L.D., Hanna, N.N., Sharma, S., 2005. Uterine NK cells mediate inflammation-induced fetal demise in IL-10-null mice. J. Immunol. 175, 4084–4090.
Myerson, D., Parkin, R.K., Benirschke, K., Tschetter, C.N., Hyde, S.R., 2006. The pathogenesis of villitis of unknown etiology: analysis with a new conjoint immunohistochemistry-in situ hybridization procedure to identify specific maternal and fetal cells. Pedia Dev. Pathol. 9, 257–265.
Nagaeva, O., Jonsson, L., Mincheva-Nilsson, L., 2002. Dominant IL-10 and TGF-beta mRNA expression in gammadeltaT cells of human early pregnancy decidua suggests immunoregulatory potential. Am. J. Reprod. Immunol. 48, 9–17.
Naik, A.K., Tandan, S.K., Dudhgaonkar, S.P., Jadhav, S.H., Kataria, M., Prakash, V.R., Kumar, D., 2006. Role of oxidative stress in pathophysiology of peripheral neuropathy and modulation by N-acetyl-L-cysteine in rats. Eur. J. Pain. 10, 573–579.
National Research Council (US) Safe Drinking Water Committee, 1986. Dose-route extrapolations: using inhalation toxicity data to set drinking water limits. In: Thomas, R.D. (Ed.), Drinking Water and Health. National Academies Press, Washington DC.
Ohoka, N., Yoshii, S., Hattori, T., Onozaki, K., Hayashi, H., 2005. TRB3, a novel ER stress-inducible gene, is induced via ATF4-CHOP pathway and is involved in cell death. EMBO J. 24, 1243–1255.
Okada, T., Yoshida, H., Akazawa, R., Negishi, M., Mori, K., 2002. Distinct roles of activating transcription factor 6 (ATF6) and double-stranded RNA-activated protein kinase-like endoplasmic reticulum kinase (PERK) in transcription during the mammalian unfolded protein response. Biochem. J. 366, 585–594.
Ord, D., Ord, T., 2005. Characterization of human NIPK (TRB3, SKIP3) gene activation in stressful conditions. Biochem Biophys. Res Commun. 330, 210–218.
Pakos-Zebrucka, K., Koryga, I., Mnich, K., Ljujic, M., Samali, A., Gorman, A.M., 2016. The integrated stress response. EMBO Rep. 17, 1374–1395.
Pinget, G.V., Corpuz, T.M., Stolp, J., Lousberg, E.L., Diener, K.R., Robertson, S.A., Sprent, J., Webster, K.E., 2016. The majority of murine gammadelta T cells at the maternal-fetal interface in pregnancy produce IL-17. Immunol. Cell Biol. 94, 623–630.
Prout, M.S., Provan, W.M., Green, T., 1985. Species differences in response to trichloroethylene. I. Pharmacokinetics in rats and mice. Toxicol. Appl. Pharm. 79, 389–400.
Purvis, H.A., Anderson, A.E., Young, D.A., Isaacs, J.D., Hilkens, C.M., 2014. A negative feedback loop mediated by STAT3 limits human Th17 responses. J. Immunol. 193, 1142–1150.
R Core Team. 2019. R: A language and environment for statistical computing. R Foundation forStatistical Computing, Vienna, Austria.
Redline, R.W., Patterson, P., 1993. Villitis of unknown etiology is associated with major infiltration of fetal tissue by maternal inflammatory cells. Am. J. Pathol. 143, 473–479.
Reis, A.S., Barboza, R., Murillo, O., Barateiro, A., Peixoto, E.P.M., Lima, F.A., Gomes, V. M., Dombrowski, J.G., Leal, V.N.C., Araujo, F., Bandeira, C.L., Araujo, R.B.D., Neres, R., Souza, R.M., Costa, F.T.M., Pontillo, A., Bevilacqua, E., Wrenger, C., Wunderlich, G., Palmisano, G., Labriola, L., Bortoluci, K.R., Penha-Goncalves, C., Goncalves, L.A., Epiphanio, S., Marinho, C.R.F., 2020. Inflammasome activation and IL-1 signaling during placental malaria induce poor pregnancy outcomes. Sci. Adv. 6, eaax6346.
Risso, D., Ngai, J., Speed, T.P., Dudoit, S., 2014. Normalization of RNA-seq data using factor analysis of control genes or samples. Nat. Biotechnol. 32, 896–902.
Romero, R., Mazor, M., Tartakovsky, B., 1991. Systemic administration of interleukin-1 induces preterm parturition in mice. Am. J. Obstet. Gynecol. 165, 969–971.
Ruckart, P.Z., Bove, F.J., Maslia, M., 2014. Evaluation of contaminated drinking water and preterm birth, small for gestational age, and birth weight at Marine Corps Base Camp Lejeune, North Carolina: a cross-sectional study. Environ. Health 13, 99.
Rushworth, G.F., Megson, I.L., 2014. Existing and potential therapeutic uses for N-acetylcysteine: the need for conversion to intracellular glutathione for antioxidant benefits. Pharm. Ther. 141, 150–159.
Rutkowski, D.T., Arnold, S.M., Miller, C.N., Wu, J., Li, J., Gunnison, K.M., Mori, K., Sadighi Akha, A.A., Raden, D., Kaufman, R.J., 2006. Adaptation to ER stress is mediated by differential stabilities of pro-survival and pro-apoptotic mRNAs and proteins. PLoS Biol. 4, e374.
Sartor, M.A., Leikauf, G.D., Medvedovic, M., 2009. LRpath: a logistic regression approach for identifying enriched biological groups in gene expression data. Bioinformatics 25, 211–217.
Seegal, R.F., Brosch, K.O., Okoniewski, R.J., 1997. Effects of in utero and lactational exposure of the laboratory rat to 2,4,2′,4′- and 3,4,3′,4′-tetrachlorobiphenyl on dopamine function. Toxicol. Appl. Pharm. 146, 95–103.
Sferruzzi-Perri, A.N., Higgins, J.S., Vaughan, O.R., Murray, A.J., Fowden, A.L., 2019. Placental mitochondria adapt developmentally and in response to hypoxia to support fetal growth. Proc. Natl. Acad. Sci. USA 116, 1621–1626.
Shahripour, R.B., Harrigan, M.R., Alexandrov, A.V., 2014. N-acetylcysteine (NAC) in neurological disorders: mechanisms of action and therapeutic opportunities. Brain Behav. 4, 108–122.
Silverpil, E., Wright, A.K., Hansson, M., Jirholt, P., Henningsson, L., Smith, M.E., Gordon, S.B., Iwakura, Y., Gjertsson, I., Glader, P., Linden, A., 2013. Negative feedback on IL-23 exerted by IL-17A during pulmonary inflammation. Innate Immun. 19, 479–492.
Soares, M.J., Chakraborty, D., Karim Rumi, M.A., Konno, T., Renaud, S.J., 2012. Rat placentation: an experimental model for investigating the hemochorial maternal-fetal interface. Placenta 33, 233–243.
Solano, M.E., 2019. Decidual immune cells: guardians of human pregnancies. Best. Pr. Res Clin. Obstet. Gynaecol. 60, 3–16.
Sprong, R.C., Winkelhuyzen-Janssen, A.M., Aarsman, C.J., van Oirschot, J.F., van der Bruggen, T., van Asbeck, B.S., 1998. Low-dose N-acetylcysteine protects rats against endotoxin-mediated oxidative stress, but high-dose increases mortality. Am. J. Respir. Crit. Care Med. 157, 1283–1293.
Su, A.L., Loch-Caruso, R., 2020. Comparison of rat fetal sex determination using placental gDNA and mRNA via qRT-PCR. J. Mol. Biol. Methods 2, 1–12.
Su, A.L., Lash, L.H., Bergin, I.L., Bjork, F., Loch-Caruso, R., 2021. N-Acetyl-L-cysteine and aminooxyacetic acid differentially modulate trichloroethylene reproductive toxicity via metabolism in Wistar rats. Arch. Toxicol.
Su, A.L., Harris, S.M., Elkin, E.R., Karnovsky, A., Colacino, J.A., Loch-Caruso, R., 2022. Trichloroethylene modifies energy metabolites in the amniotic fluid of Wistar rats. Reprod. Toxicol. 109, 80–92.
Supek, F., Bosnjak, M., Skunca, N., Smuc, T., 2011. REVIGO summarizes and visualizes long lists of gene ontology terms. PloS One 6, e21800.
Suzuki, T., Hiromatsu, K., Ando, Y., Okamoto, T., Tomoda, Y., Yoshikai, Y., 1995. Regulatory role of gamma delta T cells in uterine intraepithelial lymphocytes in maternal antifetal immune response. J. Immunol. 154, 4476–4484.
Than, N.G., Hahn, S., Rossi, S.W., Szekeres-Bartho, J., 2019. Editorial: fetal-maternal immune interactions in pregnancy. Front Immunol. 10, 2729.
U.S. EPA (Environmental Protection Agency). 2019a. Superfund: National Priorities List (NPL).
U.S. EPA (Environmental Protection Agency). 2019b. TRI Explorer (2018 Updated Dataset (released October 2019)) [Internet database]. United States Environmental Protection Agency.
van de Water, B., Zoetewey, J.P., de Bont, H.J., Mulder, G.J., Nagelkerke, J.F., 1993. The relationship between intracellular Ca2+ and the mitochondrial membrane potential in isolated proximal tubular cells from rat kidney exposed to the nephrotoxin 1,2-dichlorovinyl-cysteine. Biochem. Pharm. 45, 2259–2267.
van de Water, B., Zoeteweij, J.P., de Bont, H.J., Mulder, G.J., Nagelkerke, J.F., 1994. Role of mitochondrial Ca2+ in the oxidative stress-induced dissipation of the mitochondrial membrane potential. Studies in isolated proximal tubular cells using the nephrotoxin 1,2-dichlorovinyl-L-cysteine. J. Biol. Chem. 269, 14546–14552.
Waters, E.M., Gerstner, H.B., Huff, J.E., 1977. Trichloroethylene. I. An overview. J. Toxicol. Environ. Health 2, 671–707.
Wortel, I.M.N., van der Meer, L.T., Kilberg, M.S., van Leeuwen, F.N., 2017. Surviving stress: modulation of ATF4-mediated stress responses in normal and malignant cells. Trends Endocrinol. Metab. 28, 794–806.
Xu, F., Papanayotou, I., Putt, D.A., Wang, J., Lash, L.H., 2008. Role of mitochondrial dysfunction in cellular responses to S-(1,2-dichlorovinyl)-L-cysteine in primary cultures of human proximal tubular cells. Biochem. Pharm. 76, 552–567.
Yu, Y., Fuscoe, J.C., Zhao, C., Guo, C., Jia, M., Qing, T., Bannon, D.I., Lancashire, L., Bao, W., Du, T., Luo, H., Su, Z., Jones, W.D., Moland, C.L., Branham, W.S., Qian, F., Ning, B., Li, Y., Hong, H., Guo, L., Mei, N., Shi, T., Wang, K.Y., Wolfinger, R.D., Nikolsky, Y., Walker, S.J., Duerksen-Hughes, P., Mason, C.E., Tong, W., Thierry-

Mieg, J., Thierry-Mieg, D., Shi, L., Wang, C., 2014. A rat RNA-Seq transcriptomic BodyMap across 11 organs and 4 developmental stages. Nat. Commun. 5, 3230.